

HIGH GAIN 2D PRINTED ANTENNA ARRAY

Nethini Thilanga Weerathunge

Bachelor of Engineering
Electronic Engineering Major



Department of Electronic Engineering
Macquarie University

November,06 2017

Supervisors: Prof. Karu Esella, Mr. Muhammad Afzal



ACKNOWLEDGMENTS

I would like to express my sincere gratitude to my supervisor Prof. Karu Esella and Co-supervisor Mr.Muhammad Afzal for their guidance and encouragement in carrying out this project work.



STATEMENT OF CANDIDATE

I, Nethini Thilanga Weerathunge, declare that this report, submitted as part of the requirement for the award of Bachelor of Engineering in the Department of Electronic Engineering, Macquarie University, is entirely my own work unless otherwise referenced or acknowledged. This document has not been submitted for qualification or assessment at any academic institution.

Student's Name: Nethini Thilanga Weerathunge

Student's Signature: NETHINI

Date: 05.11.2017



ABSTRACT

Microstrip patch antennas play a vital role in wireless telecommunication due to their unbeatable qualities such as thin planar profile and low cost. There are many studies being conducted to investigate whether they can be used for long distance telecommunication such as for spacecrafts and satellites. In order to communicate between long distances the antenna should have a large gain and directivity. The directivity of patch antennas can be improved by arranging them in an array. The gain of an antenna array increases with the number of antenna elements. The reflection coefficient determines how well an antenna is impedance matched. It ensures that the reflected power by patch antenna is at a low level such that it has a high efficiency. In addition, farfield patterns indicate the side lobe levels and the beam width of the antennas radiation pattern. This project designed a 3D model of a 4×4 array with improved gain and directivity. The array is fed by a corporate feed network consists of quarter wavelength transformers in order to match the impedances. The CST software was used for all the designing and simulation purposes of antenna array. It provides different optimizer tools to tune the array to achieve desired results. The reflection coefficient, voltage standing wave ratio, farfield pattern were used to examine the performance of the array.



Contents

Acknowledgments	iii
Abstract	vii
Table of Contents	ix
List of Figures	xi
List of Tables	xv
1 Introduction	1
1.1 Scope and design specifications	3
1.2 Project overview	4
1.3 Timeline review	5
2 Background and Related Work	7
2.1 Micro-strip patch antennas	7
2.2 Feed network design	9
3 Properties of microstrip patch antennas and definitions	13
3.1 properties of micro-strip patch antennas	13
3.1.1 Dimensions of patch antennas	13
3.1.2 Impedance variation of a patch antenna	14
3.1.3 substrate permittivity	14
3.1.4 Impedance of microstrip lines	14
3.1.5 Feeding Techniques for patch antennas	15
3.1.6 Operating Frequency	19
3.2 Antenna arrays and feed networks	19
3.2.1 Corporate Feed Network	19
3.2.2 Inline Series Feed Network	20
3.3 Definitions	20
3.3.1 Directivity of an antenna	20
3.3.2 Antenna Gain	21
3.3.3 Antenna efficiency	22

3.3.4	Radiation Pattern	22
3.3.5	Far Field and Near Field	24
3.3.6	Reflection coefficient (S11)	24
3.3.7	VSWR (Voltage Standing Wave Ratio)	25
3.3.8	Smith charts	27
3.3.9	CST software	27
4	Single Patch Antenna and Feed Network design	29
4.1	Single patch antenna antenna	29
4.1.1	shapes of patch antennas	30
4.1.2	probe feed technique	30
4.2	Far-Field Arrays	32
4.3	Ideal patch antenna array design	35
4.4	Feed network design	37
4.4.1	Two Way Splitter feed network design 1	38
4.4.2	Two Way Splitter Feed network design 2	40
5	Development of Patch Antenna Array	43
5.1	Single patch antenna with an edge feed	43
5.1.1	simulation Results	44
5.2	The 2×1 array design	48
5.2.1	simulation results	49
5.3	The 2×2 array design	51
5.3.1	Simulation results	53
5.4	The 2×4 array design	54
5.4.1	Simulation results	55
5.5	The 4×4 array design	57
5.5.1	Simulation results	57
5.5.2	The 4×4 array with wave-guide port	62
5.6	Prototyping and testing	64
5.6.1	Budgetary constrains	65
5.6.2	Anechoic Chamber	67
6	Beam Steering	69
6.1	Simulation results	70
7	Conclusions and Future Work	75
7.1	Conclusion	75
7.2	Future Work	76
8	Abbreviations	79
A	Attendance Form	81

List of Figures

1.1	Large planar antenna array of Russian air defence radar [5]	2
1.2	Micro-strip patch antenna array [6]	2
1.3	Communication distance depends on the gain of the antenna array	2
1.4	Estimated Timeline	5
1.5	Realized Timeline	6
2.1	Patch antenna with H and E slots [9]	8
2.2	Fabtricated four element array with slots [10]	8
2.3	16 element antenna array [11]	9
2.4	Feeding network of the array [13]	10
2.5	Schematic of a single-feed switchable feed network [14]	11
2.6	Butler matrix block diagram [12]	11
3.1	Edge feed [24]	15
3.2	Quarter Wave transformer	16
3.3	Inset feed [24]	16
3.4	Coaxial Feed [24]	17
3.5	Coupled Feed [24]	18
3.6	Aperture Feeds [24]	18
3.7	Corporate Feed Network [17]	20
3.8	Inline Series Feed Network	20
3.9	Radiation pattern of an antenna	23
3.10	Far Field and Near Field of an antenna	24
3.11	Two port system	25
3.12	Voltage Measured along a transmission line	26
4.1	Single patch antenna design	29
4.2	Common shapes of patch antennas [19]	30
4.3	Patch Antenna Element	31
4.4	Probe Feed technique	31
4.5	Reflection coefficient of single patch	32
4.6	Radiation pattern in Cartesian plane	32
4.7	Radiation pattern in 3D plane	33
4.8	VSWR result for patch antenna	33

4.9	Gain of the 4×4 array for λ_0 elemnt spacing	34
4.10	Radiation pattern of the 4×4 array for $\lambda_0/2$ spacing	35
4.11	Symmetrical radiation pattern of the 4×4 array for $\lambda_0/2$ spacing	35
4.12	Radiation pattern of 4×1 array for λ_0 spacing	36
4.13	Radiation pattern of 4×1 array for $\lambda_0/2$ spacing	36
4.14	Radiation pattern of 3×3 array for $\lambda_0/2$ spacing	37
4.15	Ideal 4×4 patch antenna array	37
4.16	Radiation pattern of the ideal antenna array	38
4.17	Two way splitter feed network 1	39
4.18	S parameters of the Two way splitter 1	40
4.19	3D Radiation pattern	41
4.20	Smith chart	41
4.21	Two Way Splitter Feed Network 2	42
4.22	Radiation pattern of the two way splitter feed network 2	42
5.1	Single patch antenna with quarter wavelength transformer	44
5.2	Reflection coefficient (S11) of patch antenna	45
5.3	VSWR simulation results	45
5.4	Radiation patten in Cartesian plan	46
5.5	3D radiation patten of the antenna	46
5.6	Tangential E-filed pattern	47
5.7	E_x component of the E-filed	47
5.8	E_y component of the E-filed	47
5.9	Direction of E-filed	48
5.10	Direction of h-filed	48
5.11	3D model of the array	49
5.12	Reflection coefficient(S11)	50
5.13	VSWR of the antenna array	50
5.14	3D radiation pattern of the array	51
5.15	Cartesian form of the radiation pattern	51
5.16	The array designed by mirroring 2×1 array	52
5.17	The finalized 3D model of the 2×2 array	52
5.18	Reflection coefficient(S11)	53
5.19	VSWR of the antenna array	53
5.20	Cartesian form of the radiation pattern	54
5.21	3D radiation pattern of the array	54
5.22	Finalized 3D model of the array	55
5.23	Reflection coefficient at 11 GHz	55
5.24	VSWR of the array at 11 GHz	56
5.25	Directivity of the antenna array	56
5.26	Realized gain of the array	57
5.27	The 3D model of the 2×2 array and element spacing	58
5.28	Reflection coefficient (S11) of the array 11 GHz	58

5.29	The voltage standing wave ratio (VSWR) of the array	59
5.30	Real impedance of the array at 11 GHz	59
5.31	Imaginary impedance of the array at 11 GHz	60
5.32	Directivity of the antenna array	60
5.33	Realized gain at 11 GHz	61
5.34	Unsymmetrical radiation from the edge of the antenna and resulting side lobe	62
5.35	Power flow of the antenna array	63
5.36	Co and Cross polarization along $\phi=0$ direction	63
5.37	Co and Cross polarization along $\phi=90$ deg. direction	64
5.38	Antenna array with waveguide port	64
5.39	Reflection coefficient at 11 GHz	65
5.40	VSWR at 11 GHz	65
5.41	Directivity of the array at 11 GHz	66
5.42	Realized gain of the array at 11 GHz	66
5.43	Anechoic Chamber [30]	67
6.1	1D beam steering antenna array	70
6.2	Cartesian form of the radiation pattern without beam steering	71
6.3	Initial 3D radiation pattern without beam steering	71
6.4	Shifted main lobe when $\theta=+16$ deg	72
6.5	Beam steering when $\theta=+16$ deg	72
6.6	Shifted main lobe when $\theta=-16$ deg	73
6.7	Beam steering when $\theta=-16$ deg	73
6.8	Steering of the E-field	74
6.9	Phased antenna array [24]	74
7.1	Mitered bend technique	77



List of Tables

4.1	Parameters List of the Patch Antenna	31
4.2	Parameters List of Two Way Splitter Feed Network 1	39
4.3	Parameters List of Two Way Splitter Feed Network 2	40



Chapter 1

Introduction

The wireless telecommunication is one of the fabulous ideas which were witnessed by the history of telecommunication technology. It plays a major role in recent telecommunication trends such as space explorations, 4G and 5G networks and wireless power transfer. The studies carried on wireless technologies are highly concentrate on the high standard of data transfer, low cost of fabrication and energy efficient protocols. As examples, wireless power transfer requires a high directivity to reduce the wastage into unwanted directions; access networks use a narrow beam of radiation to reduce the wastage of energy and to increase data security. Although a wide beam of radiation covers a large geographical area, it causes a great amount of energy loss and decrement in the amount of data that can be transferred. This situation can be mitigated by using a large amount of narrow beams instead of fewer wide beams. A narrow beam of radiation concentrates radiation in to a small area while improving the directivity and the amount of data that can be transferred. This research aims to design a high gain 2D printed antenna array to demonstrate focused transmitter and receiver for such energy-efficient wireless systems.

In general an antenna is defined as an interface between guided medium and free space which can transform electrical power into signals or vice versa [4]. They are used in radio transmitter and receiver. The transmitter provides an alternative current of desired frequency to the antenna. Then antenna converts it to an electromagnetic wave and radiates it into a specified direction. At the receiver, the antenna converts the electromagnetic wave back in to a small voltage. An array is a collection of such antenna elements that act as a single antenna [1] (Figure 1.1 and Figure 1.2). These arrays are categorized into two major types; active and passive arrays. The goal of this project is to design a passive antenna array which does not include any active elements. In a passive array antenna elements are connected to a single transmitter/receiver using a feed network [4]. At the transmission end, the electromagnetic waves generated by each element of the antenna array are superimposed with each other [4]. It can be design, such that these waves interfere constructively to improve the data transferred in to a desired direction. They will interfere destructively in to other directions to reduce the energy wastage.



Figure 1.1: Large planar antenna array of Russian air defence radar [5]

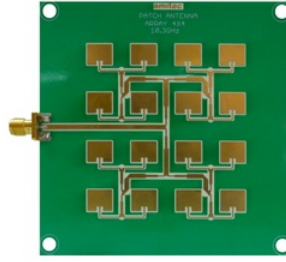


Figure 1.2: Micro-strip patch antenna array [6]

The transmitting distance of an antenna depends on its gain. If the gain is high the electromagnetic wave can travel a larger distance with lesser amount of decaying (Figure 1.3). So if the antenna has a high gain, it can be used for long distance communication [3]. Usually gain is measured in dBi or dBic. The frequency of the electromagnetic wave determines the amount of data that can be transmitted. If it has a high frequency, more data can be transmitted as signal oscillates faster such that more cycles are generated with a given period of time.

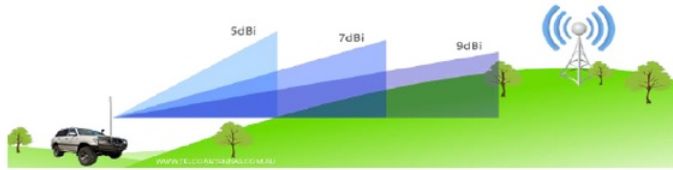


Figure 1.3: Communication distance depends on the gain of the antenna array

A higher directivity gain can be obtained by narrow beams of radiation of an antenna array compared to a single antenna. The radiation pattern consists of a main lobe and series of side lobes [2]. Main lobe holds the strongest radiation level which is directed to desired direction. Side lobes are weaker beams of radiation into other directions. It is expected to make the main lobe narrower and minimize the level of side lobes to increase the efficiency of an antenna array [2].

This research investigates on the capability of printed antenna arrays for long distance communication. It uses micro-strips to design antenna elements and the feed network. Printed antennas also called as micro-strip antennas as they are fabricated on printed circuit board (PCB) using micro-strip lines [6]. A micro-strip is a conducting strip which is separated from the ground plane by a substrate (Figure 1.2). These micro-strip antennas are commonly used in microwave frequencies. A patch antenna is a single element

of a printed antenna array. It is a patch made of a metal foil in various shapes on the surface of PCB. A 2D micro-strip antenna array consists of such micro-strip patches in a two dimensional array. Each antenna element is connected to a transmitter (or receiver) using a feed network made of micro-strip foil lines [6].

Micro-strip patch antennas are widely used in new applications due to their unbeatable qualities. These antennas have a high demand from air crafts and missiles due to their thin planar profile [1]. So they can be easily applicable on to the surface of any object while saving space. Also micro-strip patch antennas can be easily integrated on PCB with the rest of the circuit using printed circuit techniques [1]. They can be converted in to active antennas by adding elements such as microwave integrated circuits. Furthermore these antenna arrays used for military purposes such as phased array radars that are required to have a high performance [6]. These high gain antennas provide a path to MIMO (multiple-input and multiple-output) increasing its reliability to overcome the interferences of the signals from unwanted directions. In addition they are used to steer the beams from different directions to a single point. The most common applications of micro-strip patch antenna arrays include broadcasting, beam forming, naval purposes, radio frequency identification, optical phased arrays, weather forecasting, missile guidance and mobile communication [1]. In addition, satellite communication uses circular or rectangular patches as desired. Global positioning satellite systems (GPS) uses circular polarized micro-strip antenna arrays. Wearable micro-strip patch antennas are used in telemedicine applications such as continuous monitoring of biometric data [1]. They are made of textile materials such that they can be comfortably worn for a long time. These wearable antennas can also be used for recreation, fire-fighting and wireless energy harvesting. Patch radiators are recommended for treating malignant tumours due to their light weight and ease of handle. Furthermore there are many experiments going on to investigate the possibility of using micro-strip patch antennas to communicate between Earth and space vehicles. Scientists of NASA are currently working on a patch antenna array which will allow Mars 2020 rover to communicate with Earth directly without using a repeater antenna in the middle [7].

1.1 Scope and design specifications

This project aims to design a 3D model of a 4×4 micro-strip patch antenna array that has a high gain and directivity. It mainly aims to improve the directivity and the gain of the antenna by reducing side lobe levels. The basic design requirements of the antenna array can be briefly explained as follows;

- Directivity: This antenna array targets for long distance telecommunication applications such as drones. Therefore it aims to achieve a high directivity as much as possible.

- Cost: The budget allocated for this project is AUD 400. The approvals from head of the department and project supervisors are required if the cost exceeds the limit of the budget.
- Reflection coefficient: The efficiency of the antenna array can be improved by minimizing the power reflected back from patch antennas. It is required to have a reflection coefficient of -10 dB or less at the operating frequency of the array. It ensure that most of the power delivered is received by the antenna elements
- Operating frequency: The antenna array is expected to be operated within X band (8-12 GHz) with centre frequency of 11 GHz. Therefore all the antenna designs were implemented by considering 11 GHz as the operating frequency.
- The number of elements: This antenna array consists of 16 micro-strip patch antennas to obtain a high gain
- Size: The antenna arrays is expected to have a small size to improve the area efficiency.
- substrate: Rogers RT5880 is used as the substrate (thickness=1.57 mm).

1.2 Project overview

As the first step of the project, a single patch antenna was designed and simulated to identify its dimensions in order to operate at 11 GHZ. Then this single patch antenna was used for investigate some farfield arrays. The aim was to select the most suitable spacing between antenna elements to achieve a high gain and directivity. Then an ideal 4×4 array was implemented using selected element spacing to examine the gain and directivity. In the next stage, some two way splitters were designed to get an idea about the behaviour of quarter wavelength transformers in feed networks. The 4×4 antenna array was developed in 5 stages. First a single patch antenna was designed in CST with an edge feed. Then a 2×1 array was implanted using two of such antenna elements. The design parameters of the array were tuned in order to get impedance matching at its operating frequency. Its gain, directivity, side lobe levels and other characteristic were investigated using simulation results. Likewise, a 2×2 , 2×4 and 4×4 arrays were designed in each stage. Each array was implemented based on the previous array design. Also the simulation results of each stage were used to make decisions on the next stage of the antenna array. As the fabrication of the antenna was omitted, the project was extended to investigate about beam steering. The beam steering of an antenna array was examined using a 1D antenna array with 4 patch antennas.

1.3 Timeline review

This project was conducted throughout the second semester of 2017 which is from 31st of July to 6th of November. But the timeline of the project includes both winter vacation and the mid semester break. The most of the time of winter break was allocated to get familiar with the CST software and to study basic antenna theories. Then the initial 3D modeling and EM simulations of antenna array were commenced from the beginning of the second semester. All the designing and simulations of the antenna array was done in the campus due to licensing of CST software. The laboratory and research area access was granted after conducting a safety induction. The fig.1.4 and fig.1.5 shows the estimated and realised timelines of the project up to final report submission. The timeline has given as a table instead of a Gantt chart as it is more readable in the report. The final tasks of the project will be the presentation and demonstration of the antenna array design which will be on 20th of November. In addition, the timeline was constantly updated to meet various constrains. This was very important as each antenna design was built on the previous stage.

The major milestones/tasks of the project has outlined in the fig.1.5. Some planed tasks such as fabrication and testing had to be removed due to technical constrains. Also the order of some tasks had to be changed as they take more time than expected. However, the project could be completed earlier than expected because it was decided not to the prototyping. So the project was extended to investigate about beam steering of simple 1D antenna arrays.

Tasks	Time allocation					
	June	July	Aug	Sep	Oct	Nov.
Studying basic antenna theories	■					
Learning CST software	■	■				
Single patch antenna design with a port		■				
Fairfield array simulations		■	■			
Ideal array design			■			
Two way splitter designing			■	■		
Single patch antenna with edge feed				■		
2×1 antenna array				■	■	
2×2 antenna array					■	
2×4 antenna array					■	
4×4 antenna array					■	
Prototyping and testing					■	■
Final report preparation					■	■

Figure 1.4: Estimated Timeline

Tasks	Time allocation					
	June	July	Aug	Sep	Oct	Nov.
Studying basic antenna theories	■	■				
Learning CST software	■	■				
Single patch antenna design with a port		■				
Fairfield array simulations			■			
Ideal array design			■			
Two way splitter designing			■			
Single patch antenna with edge feed				■		
2×1 antenna array				■		
2×2 antenna array				■		
2×4 antenna array					■	
4×4 antenna array					■	
Beam steering antenna array					■	
Final report preparation					■	

Figure 1.5: Realized Timeline

Chapter 2

Background and Related Work

Although the concept of micro-strip patch antennas started in 1950s, it couldn't attract significant attention until 1970s [8]. Since then this technology developed gradually such that it plays a major role in today's telecommunication industry. With the development of space exploration and mobile telecommunication (4G and 5G), many experiments have carried out to increase the capability of long distance communication and the gain of antennas. This section illustrates some background work that relates to this research project. The designing of the antenna array can be divided in to two parts namely designing of patch antennas and designing of the feed network. So, previous studies of micro-strip patch antennas will be discussed in two sections.

2.1 Micro-strip patch antennas

J.saini and S.K. Agarawal, have done a research on a micro-strip patch antenna which can be used in future 5G applications [9]. The antenna has simulated on Rogers RT5880 substrate using CST software. It has a maximum gain of 5.42 dB at 60 GHz frequency. This design has a H slot and an E slot on the patch which enhance the impedance (Figure 2.1) [9]. Simulations have shown that this H and E slots have enhanced the impedance bandwidth compared to a reference antenna. In addition this design uses micro-strip line as the feed line.

The research conducted by D. Prabhakar and Et al, has also used multiple U slots to improve the impedance bandwidth [10]. Loading suitable slots with radiation edges of patch can also improve the bandwidth. Slots bring dual band properties in the patch antenna by disturbing the path of the current. The reason of using U shaped slots for this design is because they are relatively simple design. Also this type of slot design does not use stacked or coplanar parasitic patches which increase the thickness or the size of the antenna [10]. Sometimes more than one resonant frequency may be obtained while enhancing the impedance bandwidth. The loading of slots on the patch increase the current length. The increment of the current length results in lowering fundamental resonance

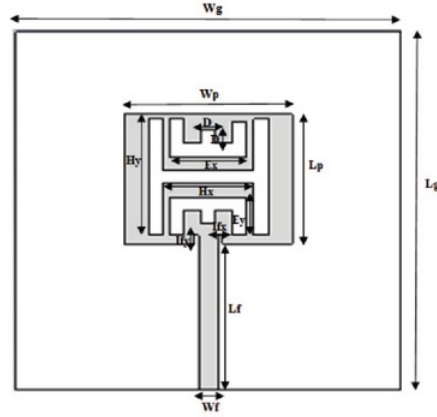


Figure 2.1: Patch antenna with H and E slots [9]

frequency that corresponds to reduced antenna size. This antenna array design has used a slot of 10 mm at the centre of the patch and four slots of 4 mm around the four corners (Figure 2.2). The array has designed on FR4-epoxy substrate and has simulated using Metered bend feed network. Its maximum reflection coefficient is -34.92 at 3.26 GHz. Maximum gain has obtained as 9.65 dB [10].

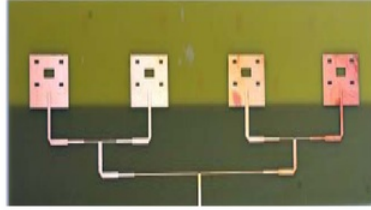


Figure 2.2: Fabricated four element array with slots [10]

Beenish and Et al propose a 16 element micro-strip patch antenna array with maximum gain of 14.82 dB for 28.5 GHz millimetre wave applications [11]. Its patches are connected in a 2D planner arrangement using micro-strip lines as feeds. Also this experiment shows that the operational frequency of the array can be shifted from 28.5 GHz to 33 GHz by varying the width of the feed lines. This array has an impedance matching of -21.7 dB and reflection coefficient of -26 dB at 28.5 GHz ad 33 GHz respectively [11]. The results of this experiment prove that an array of patch antennas with smaller and uniform dimensions is ideal to overcome the path loss effects. All the simulations of this array design have done using Ansoft HESS software. The first step of designing this array

was organizing four patches with same width and length in to a square shape to obtain a 2×2 array. Each element of 2×2 array has connected using micro-strip lines. Then 16 element array has obtained by connecting four of these 2×2 arrays (Figure 2.3). The co-axial feed that provides the array with required excitation has placed at the centre of the main array. This array design uses a single co-axial feed instead of micro-strips to avoid the radiations inside substrate [11]. According to results, authors conclude that this array is suitable for 5G mobile communication.

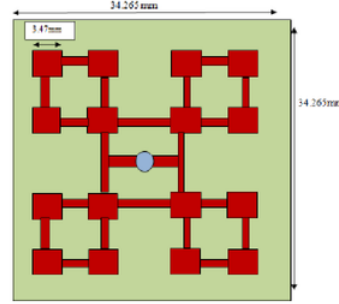


Figure 2.3: 16 element antenna array [11]

2.2 Feed network design

The common material used for feed networks of patch antennas is micro-strip lines. There are few types of feed networks namely, edge feed, parallel feed, series feed and corporate-feed. The wideband antenna array proposed by S.G. Zhou and Et al uses a full corporate-feed network (Figure 2.4). Also it has employed an air-filled micro-strip feeding network to achieve high efficiency by avoiding substrate losses [13]. In addition to air-filled transmission lines, rectangular coaxial lines have been reported as a solution for dielectric loss. This 4×4 array operates in Ku-band and has fabricated using conventional milling techniques [13]. The antenna configuration consists of four parts; cavity radiation element, the ground plane, micro-strip feeding network and back cover for the feed network. The air-filled cavity acts as the antenna element and stepped ridge is used in it to improve impedance matching. This design reduces the coupling between transmission lines by placing the micro-strip feed network within a cavity on the back cover [13]. In addition there are some cylinder supports for feeding network to achieve impedance matching. They have placed at the T junctions of the network. Finally, a microstrip-subMiniature version A (SMA) transition has provided at the end terminal of the feed network. The gain of the array varies from 18.4 dBi to 21.4 dBi within the frequency band of 10.5-14.5 GHz [13]. The actual array consists of a full metal structure. The size of the entire

structure is $80 \times 80\text{mm}$.

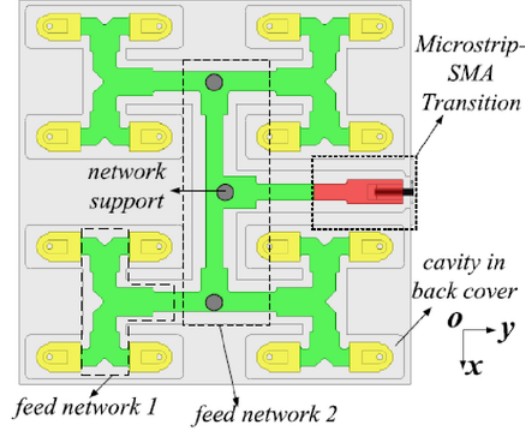


Figure 2.4: Feeding network of the array [13]

H.M. Lee has investigated about a reconfigurable micro-strip patch array antenna that uses a switchable feed-network. The switchable feed network presented in this study combines two ports of micro-strip antenna with a quarter wavelength transformer (Figure 2.5). The major assumption of the operation of switchable feed network is that a quarter wavelength feed line is terminated with a micro-strip antenna [14]. It also assume that the resonant frequency ratio of the two micro-strip patches to be close to 1.4:1. This switchable feed network can be constructed using multiple odd numbers of a quarter wave transmission line such that it can be used for a beam pattern reconfigurable antenna system. This proposed feed network design has simulated in CST software on Teflon substrate.

The proposed antenna array by O.U. Khan operates at X band at centre frequency of 8.3 GHz which is used for satellite communication [12]. The large coverage area and the high user density demand multiple spot beams instead of a single beam for satellite antennas. It increase the capacity of the system of allow to frequency reuse. In this research he has used a butler matrix to form a beam forming network that produces multiple beams. A $N \times N$ butler matrix with N number of patches generates N orthogonal beams at different locations [12]. The proposed 4×4 butler matrix consists of four 90° hybrids, two crossovers and two phase shifters (Figure 2.6). Then the matrix is used to feed circularly polarized four element antenna array. It also uses RT/Duroid 5880 substrate based on ease of availability, low cost and low radiation losses. The elements have spaced with the distance of $\lambda/2$.

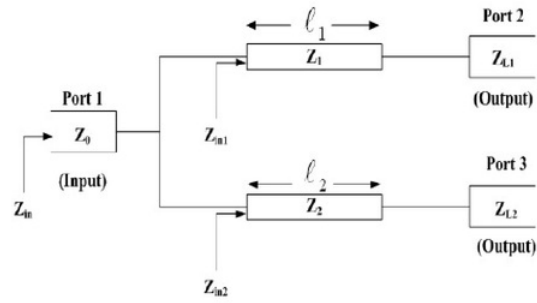


Figure 2.5: Schematic of a single-feed switchable feed network [14]

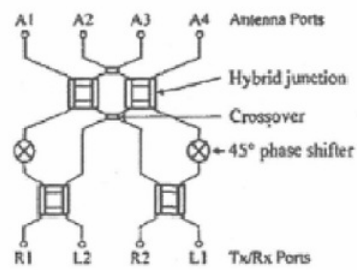


Figure 2.6: Butler matrix block diagram [12]

Chapter 3

Properties of microstrip patch antennas and definitions

The designing process of an antenna array consists of various calculations such as its dimensions, operating frequency, impedance, gain, efficiency and directivity. Different antenna types receive and transmit EM waves within different frequency ranges across the RF spectrum. These EM waves travel at a same speed as the speed of light (c) through free space (or air). The speed of an EM wave in free space can be expressed in terms of its frequency (f_0) and wavelength (λ_0) (3.1)

$$Wavelength(\lambda_0) = c \times f_0 \quad (3.1)$$

3.1 properties of micro-strip patch antennas

3.1.1 Dimensions of patch antennas

As mentioned before, a micro-strip patch antenna is a conducting strip which is separated from ground plane using a substrate. The width (W) of the patch antenna depends on the operating frequency (f_0) and dielectric constant of the substrate (ϵ_R). It can be calculated by using(3.2) where c is the speed of light in free space. The effective dielectric constant (ϵ_{eff}) of the substrate can be represent in terms of dielectric constant (ϵ_R), the height of the substrate (h) and the width of the patch (3.3). Hence the actual length of the patch can be calculated using (3.4)

$$Width(W) = \frac{c}{2 \times f_0 \sqrt{\left(\frac{\epsilon_R+1}{2}\right)}} \quad (3.2)$$

$$\epsilon_{eff} = \frac{\epsilon_R + 1}{2} + \frac{\epsilon_R - 1}{2} \left[\frac{1}{\sqrt{1 + 12\left(\frac{h}{W}\right)}} \right] \quad (3.3)$$

$$Length(L) = \frac{c}{2 \times f_0 \sqrt{\varepsilon_e f f}} - 0.824h \left(\frac{(\varepsilon_e f f + 0.3)(\frac{h}{W} + 0.264)}{\varepsilon_e f f - 0.258)(\frac{h}{W} + 0.8)} \right) \quad (3.4)$$

For ease of calculations an online calculator was used to calculate patch antenna dimensions. [15].

3.1.2 Impedance variation of a patch antenna

The impedance of a patch antenna is a major parameter that should be considered in feed network designing. The impedance of an antenna depends on its physical dimensions; width and length, operating frequency and the permittivity of the substrate. The centre of the patch antenna has the zero impedance and it increase with the distance from the centre to a given point. So the edge of the patch has the maximum impedance. When designing a feed network, it is important to match the impedance of the patch and the feed line to improve the efficiency. So the concept of VSWR has introduced to check how well the antenna is impedance matched.

3.1.3 substrate permittivity

The permittivity of the substrate that the antenna array will be built on is a critical factor when determining the dimensions of the patch antennas, feed lines and quarter wavelength transformers. The relative permittivity determines the speed of an EM wave through a substrate compared to its speed through free space (c). More importantly, the permittivity of the substrate affects the wave length of the EM wave. This varied wavelength due to the permittivity is called guided wavelength (λ_g) and it is given by 3.5. Therefore guided wavelength through the relevant substrate provides more accurate results when calculating antenna dimensions.

$$Guidedwavelength(\lambda_g) = \frac{\lambda_0}{\varepsilon} \quad (3.5)$$

In this antenna design uses RT5880 substrate which has a permittivity of 2.2, so λ_g was calculated as 18.39 mm.

3.1.4 Impedance of microstrip lines

The CST software has a built in function called Macros tool which is frequently used for calculating dimensions and impedance of micro-strip lines. It allows to find the width of

a micro-strip line in order to achieve a desired impedance. The dimensions of a micro-strip line depend on the dielectric constant of the substrate, dielectric height, operating frequency and desired line impedance. However due to ease of use, an online micro-strip line calculator was used to calculate the width and length of transmission lines. [16]

3.1.5 Feeding Techniques for patch antennas

Edge feed

In the edge feed method the antenna will be fed from one of its radiating edge(3.1). At most of the time, the edge impedance of the antenna does not match with the impedance of the micro-strip transmission line. So there must be an intermediate element that does the impedance matching. It is called a quarter-wavelength transformer which is also a microstrip line with special dimensions [29].

If the edge impedance of the microstrip patch antenna is Z_A and the impedance of the

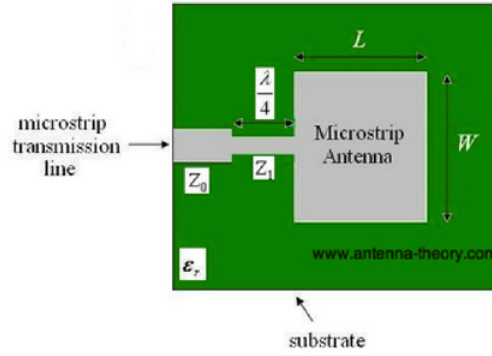


Figure 3.1: Edge feed [24]

transmission line is Z_0 , then the matching impedance of the quarter wavelength transformer (Z_1) is given by (3.6). More importantly, the length of the transformer should be $\lambda_g/4$. The width can be calculated similar to an ordinary transmission line's width.

$$Z_0 = \sqrt{Z_{in} \times Z_L} \quad (3.6)$$

The edge feed method was used as the feeding technique for each patch in this proposed antenna design.

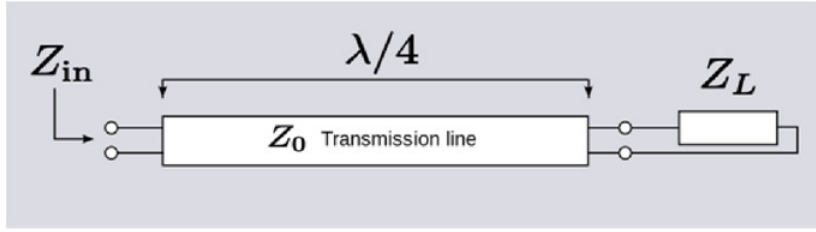


Figure 3.2: Quarter Wave transformer

Inset Feed

The one drawback of edge feed is that it typically yields high input impedance. The current flow is relatively low along the edge of the patch antenna and it increases towards the centre. This leads to a very low impedance at the centre and high impedance along the edge of the antenna. So the input impedance can be reduced by feeding closer to the centre of the patch. The method of doing this is known as the inset feed where the patch is fed at a distance R from the edge (3.3).

The current flow has a sinusoidal distribution on the antenna surface. Therefore, the

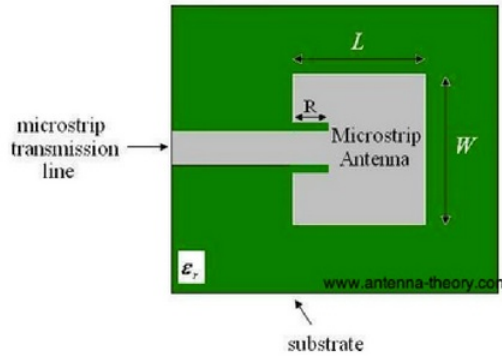


Figure 3.3: Inset feed [24]

current at point which locates distance R from the edge increases by $\cos(\pi R/L)$. It means that the wavelength becomes $2L$ and so the phase difference is $2\pi R/2L = \pi R/L$. As the current increases, the voltage decreases by the same amount. Hence, the input impedance (impedance at the desired point Z_{in}) is scaled as shown in 3.9.

$$Z_{in} = \cos^2 \frac{\pi \times R}{L} \times Z_{in}(0) \quad (3.7)$$

The $Z_{in}(0)$ is the edge impedance of the antenna. So the inset feed method can be used to obtain a desired input impedance.

Coaxial Cable/ probe Feed

Patch antennas can be fed from the bottom using a probe or a coaxial cable. The outer conductor of the cable is connected to the ground plane and its copper core is extended until the bottom of the patch antenna 3.4.

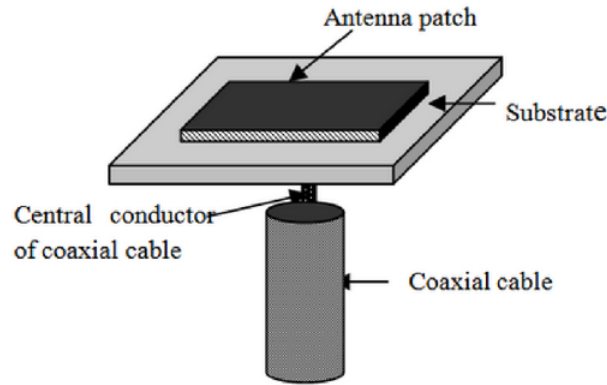


Figure 3.4: Coaxial Feed [24]

The position of the probe can be altered to obtain desired input impedance as in inset feed. Furthermore, the coaxial feed introduces an additional inductance which needs to be considered if the substrate thickness (h) increases largely. Another drawback of this method is that the probe can also radiate which causes to radiation in unwanted directions. Also this method may increase the cost of fabrication if it is used for antenna array design.

Coupled (Indirect) Feed

In this method the feed does not directly connect to the antenna. If a probe feed is considered, the copper core can be trimmed such that it does not extend up to the bottom of the patch. The inset method can also be implanted using this technique. So the inset

feed terminates just before the antenna.

This feeding method adds an extra freedom to the antenna design. Also the gap between the antenna and the transmission line generates a capacitance which helps to cancel out the inductance due to the coaxial feed 3.5.

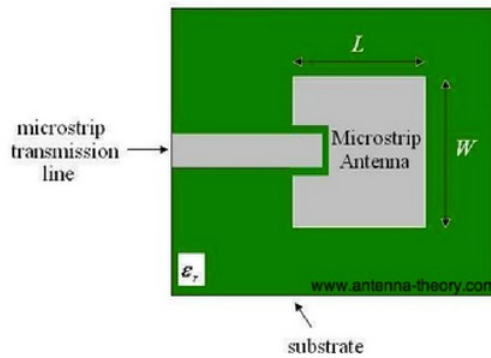


Figure 3.5: Coupled Feed [24]

Aperture Feeds

This is a feed method that shields the transmission line from the antenna using a conducting plane. But the conducting plane consists of an aperture (hole) in order to transmit energy to antenna.

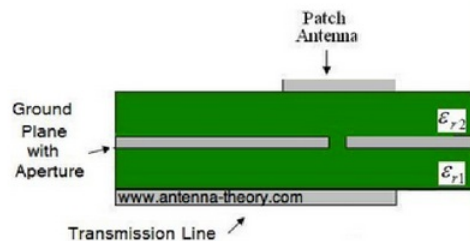


Figure 3.6: Aperture Feeds [24]

The upper layer is made of a substrate with a lower permittivity to ensure better radiation by producing loosely bound fringing fields. The lower substrate is selected to

have a high permittivity to avoid producing undesired radiation. The disadvantage of this aperture feed method is that it complicates the fabrication.

3.1.6 Operating Frequency

The operating frequency is the frequency in RF spectrum where the antenna resonates at. Therefore it is also called as resonance frequency. The designed antenna array was aimed to operate at 11 GHz which is within X-band of RF spectrum. The dimensions of each patch antenna can be calculated such that it operates at a desired frequency.

3.2 Antenna arrays and feed networks

A micro-strip antenna array is a cluster of single patch antennas which act as a single antenna. These arrays are designed in many configurations. Rectangular and circular antenna arrays can be identified as the most common antenna configurations. The rectangular array configuration is relatively simpler in terms of designing and fabrication. The proposed antenna array was implemented using this configuration. Feed network for an antenna array is a major designing concern in terms of its complexity and size. There are various kinds of feed networks depending on the type of antenna and its geometry. As mentioned before, antenna arrays are categorized into active and passive arrays. As the proposed antenna array is a passive array it is important to investigate the types of feed networks that are applied for them. There are two types of feed networks that are commonly used for passive arrays namely; corporate feed networks and Inline series feed networks.

3.2.1 Corporate Feed Network

Corporate feed networks (Fig.3.7) are the most common feeding networks for passive antenna arrays. It combines RF feed network with the patch antennas. They are designed according to a similar configuration as parallel feed networks. This feed network was used for the antenna array designed in this project. It was used as a combination of feed lines and quarter wavelength transformers. This feed network method was selected as it provides more control on power input and modifying radiation by varying feed line dimensions. Also it can be used to split input power evenly to each patch antenna by using quarter wavelength transformers and T-junctions in the feed network 3.7.

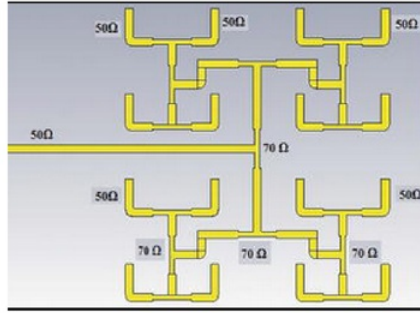


Figure 3.7: Corporate Feed Network [17]

3.2.2 Inline Series Feed Network

A series feed network is serially coupled with the antenna elements. The input signal is fed at one end of the feed network. These feed networks are more compact compared to parallel feed networks. It also reduces the radiation losses due to feed network because of its small size and efficient than corporate feed arrays. However, this feed networks suffers from major drawbacks such as narrow bandwidth and inherent phase difference. In contrast, the corporate feed networks have a well control space distribution between patches. In addition the input power for patch antennas in a corporate feed is independent of each other and can be controlled as desired.



Figure 3.8: Inline Series Feed Network

3.3 Definitions

3.3.1 Directivity of an antenna

The directivity (D) is a fundamental parameter which measures how directional the antenna radiation pattern is [24] [27]. Isotropic antenna is a hypothetical antenna that radiates radio waves with same intensity in all directions. Therefore these antennas have zero directionality and directivity of 1 (0 dB). Although isotropic antennas are hypothetical, they are used as a common reference when defining the directivity of other antenna types. The specified directivity for an antenna actually refers to the peak directivity. The directivity

is a function of angle which is described by the radiation pattern. So the directivity of an antenna is simply defined as the ratio between peak value of radiated power (U_{max}) and the average power radiated over all directions (power radiated by isotropic antennas P_{rad}).

$$D = 4 \times \pi \times \frac{U_{max}}{P_{rad}} \quad (3.8)$$

The increased directivity creates a more focused or directional antenna. These antennas are required to be many wavelengths in size. Dish antennas and horn antennas are high directivity antennas that are many wavelengths long. According to Antenna theory, an antenna has to be electrically small to generate a low directivity. The minimum of the electrical length is the quarter wavelength such that it would not affect the efficiency and the bandwidth of the antenna.

The directivity of an antenna is decided according to its application or the purpose. The antennas used for cell phones need to pick up signals from any direction so its directivity should be low. In contrast, satellite dish antennas should be capable of receiving signals from a fixed direction. Therefore they are designed to have a higher directivity. The power wastage of an antenna with a higher directivity is significantly low compared to one with a low directivity as the radiation pattern is focused to one direction [4]. The proposed antenna design also focuses on reducing the power wastage by increasing the directivity.

3.3.2 Antenna Gain

The gain of an antenna refers to the power that is transmitted in the direction of peak radiation compared to that of an isotropic antenna [24]. The gain of an antenna considers the actual losses that occur while radiating the EM waves. Therefore it is commonly quoted in antenna's data sheet than the directivity.

Throughout this antenna array design, the gain is expressed as a function of angle. In this case the radiation pattern of the antenna is plotted by using the gain as the measuring unit (magnitude of the radiation pattern).

If a transmitting antenna has a gain of 10 dB, it means that the power received far from the antenna will be 10 dB higher than the power that will be received from a lossless isotropic antenna with a same input. A lossless antenna has an efficiency of 0 dB (100%). Similarly, if a receiving antenna has a gain of 10 dB, it receives 10 dB more power than a lossless isotropic antenna.

Most commonly a single value is given as the gain of an antenna; that is its peak gain over all directions. The antenna gain (G) can be expressed in terms of directivity (D) and

antenna efficiency (ϵ) .

$$G = E \times D \quad (3.9)$$

The antenna gain is usually given in dB, dBi or dBd units.

3.3.3 Antenna efficiency

The efficiency (ϵ_R) of an antenna is the ratio between the input power (P_{input}) to the antenna and the power radiated ($P_{radiated}$) from antenna 3.10.

$$\epsilon_R = \frac{P_{radiated}}{P_{input}} \quad (3.10)$$

An antenna with high efficiency radiates most of the power present at its input. A low efficiency antenna absorbs most of its input power due to losses within the antenna or reflects back due to impedance mismatch. Therefore obtaining a good impedance match at each stage of the antenna design is important. The more important fact is that the efficiency of an antenna does not change whether it is used as a receiver or a transmitter. This concept is called antenna reciprocity. The antenna efficiency is frequently quoted as a percentage or in decibels (dB).

The efficiency addressed in equation 3.10 sometimes called as antennas radiation efficiency. In addition the term total efficiency (ϵ_T) is also used in practice. It is given by the multiplication of radiation efficiency and the impedance mismatch loss of the antenna (M_L) 3.11.

$$\epsilon_T = \epsilon_R \times M_L \quad (3.11)$$

In practice, antenna efficiency is typically referred to the total efficiency which includes the impedance mismatch loss. The efficiency of antenna reduces mainly due to finite conductivity of the metal that the antenna is made of (conductivity losses), conductivity of the dielectric material used (dielectric losses) and the impedance mismatch losses.

3.3.4 Radiation Pattern

The term radiation pattern refers to the directional (angular) dependence of the radiated power by an antenna [28]. The arrival angle that leads to the variation of radiated

power is observed from the antenna's far field. It can be represented in 3D or 2D space or in Cartesian or polar coordinates. These plots are useful in identifying the radiation direction of the antenna. When plotting the radiation pattern in 2D space, the standard spherical coordinates are used. It plots the normalized radiation pattern according to the variations of θ (Elevation angle), which is the angle measured off the z-axis and ϕ (Azimuth angle) which is the angle measured counter-clockwise off the x-axis. It should be noted that the 2D space is more suitable for simpler radiation patterns.

Plotting the radiation pattern in 3D space is ideal when the desired radiation pattern is more complex. Also it helps to identify the main lobe and the side lobes very easily. The main lobe is the lobe which has the maximum power and the greatest field strength. In a radiation pattern this main lobe falls to the zero angle. A directional antenna aims to emit the radio waves from a desired direction and to omit or reduce the radio waves coming from other directions. Therefore the lobe in that direction is intended to have higher field strength than other lobes. So it appears biggest in the graph of the radiation pattern of the antenna and is defined as the main lobe. Other lobes are called the side lobes. These side lobes usually visualize the unwanted radiation in to undesired directions. So in an antenna design, it is aimed to reduce the side lobe levels to minimize the power wastage in to undesired directions. The lobe that is located into the opposite direction of the main lobe is defined as back lobe 3.9.

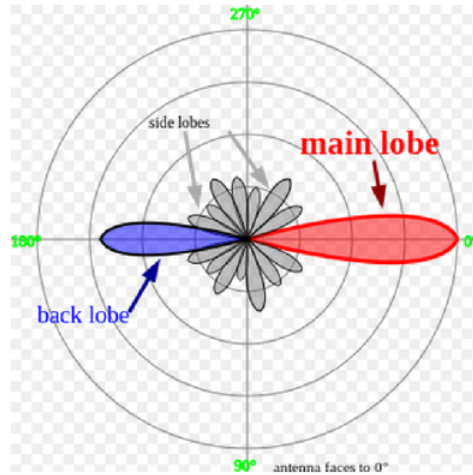


Figure 3.9: Radiation pattern of an antenna

In the antenna design, it is expected to get the radiation pattern in the broadside direction which is perpendicular to the patch. This is because the antenna has the maximum directivity in its broadside direction.

3.3.5 Far Field and Near Field

The Far field and near field 3.10 refer to the regions of electromagnetic field around a radiating object. The near field dominates close to the radiating object while Farfield dominates at greater distances. Any electromagnetic radiation has a electric field component which is given by E and a magnetic field component given by H . The relationship between these field components changes depending on the region of the electromagnetic field.

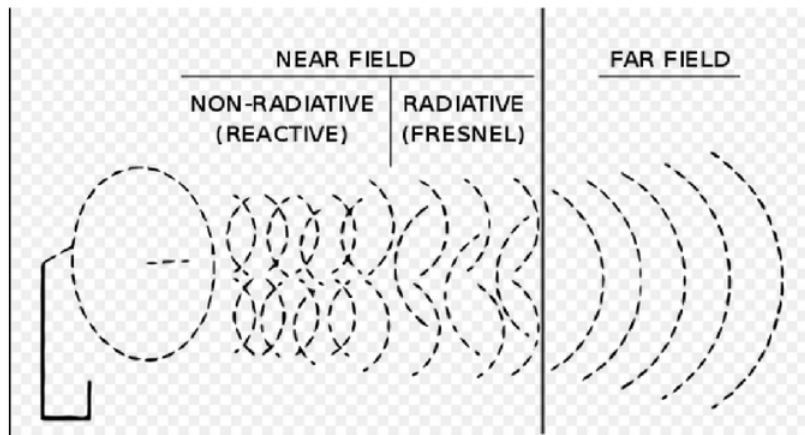


Figure 3.10: Far Field and Near Field of an antenna

Within the Farfield, a freely propagating wave has same magnitude for both E and H components at any given point on the free space. Within the near field the relationship between E and H becomes more complex. As an antenna is also a radiating component its electromagnetic field also consists of E and H components. They can be modelled using Farfield monitor of CST software.

3.3.6 Reflection coefficient (S_{11})

S parameters are highly considered when analyzing the simulation results of antenna designs. They represent the input-output relationship between the ports in an antenna system or in any electrical system. If there are two ports in the antenna system 3.11, then S_{12} means the amount of power transferred from port 2 to port 1. S_{21} represents

the power transferred from port 1 to port 2.

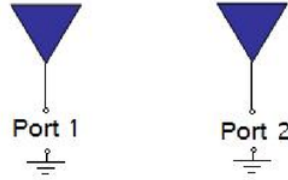


Figure 3.11: Two port system

In general a port is a terminal where both voltage and current can be delivered. In a situation where there are two radios then their terminals are the ports that deliver power to the two antennas. Therefore S_{11} is the reflected power that the radio 1 was trying to transfer to antenna 1. S_{22} is the reflected power that was transferred by radio 2 to antenna 2. The S_{12} is the power that was delivered to radio 1 through antenna 1 by radio 2. More importantly these S-parameters are defined as a function of frequency.

According to Fig.3.11, S_{21} refers to power received at antenna 2 with respect to the power input at antenna 1. If $S_{21} = 0$ dB, it means that all the input power at port 1 is ended up at port 2. Also, $S_{21} = -10$ dB means, if the input power at port 1 is 1 Watt (0 dB), then 0.1 Watts (-10 dB) is received at port 2.

In this research project, most commonly quoted S-parameter is S_{11} . S_{11} is the reflection coefficient (Γ) or return loss which represent the power reflected back from the antenna. If $S_{11} = 0$ dB, it means all the input power was reflected back and nothing radiates by the antenna. It is not desired for an antenna design. If $S_{11} = -10$ dB, this means that if the input power is 3 dB, then -7 dB is the reflected power. The rest has delivered to the antenna. This delivered power is either radiated or absorbed within the antenna. Ideally, the antennas are designed to be low loss such that most of the power delivered is expected to be radiated. When analysing the simulation results of this project it was desired to get S_{11} is less than 10 dB.

3.3.7 VSWR (Voltage Standing Wave Ratio)

Impedance matching plays a major role when observing accurate results for an antenna design. The impedance of the radio (receiver or transmitter) and the transmission line has to be well matched with that of the antenna. The VSWR is a numerical measurement that represents how well the antenna is impedance matched with the transmission line.

The voltage Standing Wave Ratio (VSWR) is defined as a function of the reflection coefficient (S_{11}/Γ). The VSWR is given by the following formula 3.12.

$$VSWR = \frac{1 + |\Gamma|}{1 - |\Gamma|} \quad (3.12)$$

This numerical value for antennas is always a real positive number. It is desired to have a smaller VSWR value which means that the antenna is impedance matched with the transmission line and more power is delivered to antenna. In an ideal case, where VSWR is 1.0, no power is reflected back from the antenna. Also this is the minimum value of VSWR.

The bandwidth requirement of antennas is commonly given in terms of VSWR. As an example if an antenna is required to operate at 500-800 MHz band with $VSWR \leq 3$, this means VSWR is less than 3 within this specified frequency range. Above specification also means that the reflection coefficient is less than 0.5 within quoted frequency range. VSWR is obtained from the measured voltage along a transmission line which leads to an antenna 3.12. It is the ratio between the peak amplitude and the minimum amplitude of a standing wave.

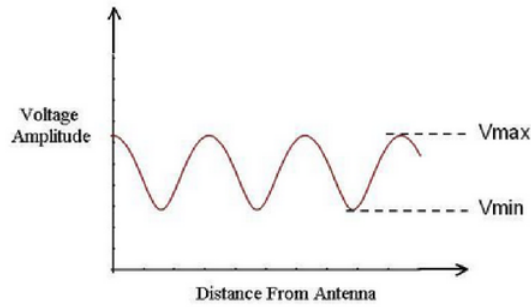


Figure 3.12: Voltage Measured along a transmission line

In industry VSWR is commonly called as vi-wer. When an antenna is not impedance matched, it causes a reflected voltage wave. This reflected wave creates standing waves along the transmission line resulting peaks and valleys (fig.2). So $VSWR=1$ means that there is no reflected power and the voltage has a constant magnitude along the transmission line.

It is considered that antennas which have VSWR less than 2 are very good. When VSWR increases two main negatives arise. The obvious problem is more amount of power

will be reflected back and less will be transmitted. The other problem is when VSWR increases, more power is reflected back in to the transmitter. This large amount of reflected power can damage the transmitter. Also transmitters will have problem in transmitting correct data bits if the antenna is poorly impedance matched.

Although VSWR measures the power delivered to antenna it does not means that all the received power will be radiated. Hence, it measures the potential to radiate. As mentioned earlier low VSWR means that the antenna is well-matched but it does not mean that all the received power will be radiated. To determine the radiated power it is required to use an anechoic chamber or other radiated antenna test. In addition VSWR can be measured on Smith charts.

3.3.8 Smith charts

Smith charts can be identified as a tool for visualizing the impedance of transmission lines and antenna systems. They also can be used to understand the behavior of transmission lines from the perspective of impedance. In this research smith charts were used to check impedance matching of antenna designs. A Smith chart displays the actual (physical) impedance of the antenna when measured on a vector Network Analyzer (VNA).

Originally, these Smith charts were developed by Phillip Smith in 1940s to simplify the calculations related with transmission line equations. Although Smith charts are not used for this purpose due to the development of modern computers, they are still been used for the visualization of the impedance of antennas or transmission lines.

A Smith chart presents complex reflection coefficient (Γ), in polar form 3.13. Where Z_L is the impedance attached to the transmission line and Z_0 is characteristic impedance.

$$\Gamma = \frac{Z_L - Z_0}{Z_L + Z_0} \quad (3.13)$$

Although VSWR is a function of the absolute value of Γ , it can also represent in Smith charts. If VSWR=1 is represented as the center of the Smith Chart, then VSWR=3 would be the circle which is centered at the origin the of Smith chart with $\Gamma=0.5$ magnitude. Therefore each circle centered at the origin of a Smith chart represents a constant VSWR. The outer boundary of the Smith chart where $\Gamma=1$, represents the VSWR of infinity.

3.3.9 CST software

In this research, all the 3D EM simulations were done in CST microwave studio. It is specialized software for EM simulations of high frequency components [26]. CST allows fast and accurate analysis of high frequency designs such as antennas, planar, filters and couplers. It provides the capability of tackling a wide range of high frequency applications using many solver technologies. The most popular solver technologies offers by CST

are flagship module, time domain solver and frequency domain solver [26]. This research project mainly uses time domain solver for analysing the antenna array.

This software allows to create the antenna design in 3D plane using x, y and z coordinates. It allows users to enter the dimensions of the elements as variable parameters. These parameters can be swept in order to find the best match for desired conditions such as impedance matching and radiation patterns. Using variables make easier to do the changes to the parameters values without changing each and every design steps. CST allows has a library of materials that can be used as the substrate for antenna designs.

Probes can be used to model the input to the antenna design and simulations can be done considering a single port or many ports.

Simulation results can be viewed in 3D space, 2D space, Cartesian plane or in polar form. These simulation results provide important characteristics such as impedance, impedance matching and reflection coefficient. Also it allows to set field monitors to visualize E-field, H-field, power, and surface current flow of the antenna.

Chapter 4

Single Patch Antenna and Feed Network design

The proposed antenna array can be addressed in terms of two subsystems namely patch antenna array and the feed network. The first design step was to design a single micro-strip patch antenna and determining its dimensions.

4.1 Single patch antenna antenna

As mentioned before, this antenna design consists of 16 micro-strip patch antennas. The very first step of the designing process involves in designing one of such antenna element. The antenna design consists of three layers; ground plane, substrate and the patch 4.1. Patch antenna and the ground plane are separated by the RT5880 substrate which has a permittivity of 2.2. Both patch antenna and the ground is implemented on copper (annealed) metal.

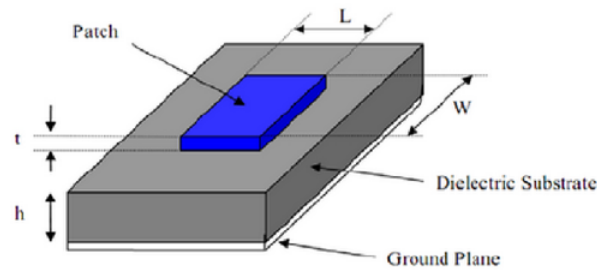


Figure 4.1: Single patch antenna design

4.1.1 shapes of patch antennas

Microstrip patch antennas can be designed in many shapes such as Rectangular, Square, circular, Dipole, Elliptical, Disc sector, Circular ring and Ring sector 4.2. Among them Rectangular, Circular and Triangular shapes can be considered as most popular ones.

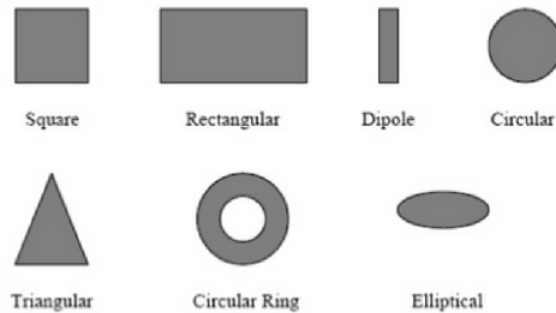


Figure 4.2: Common shapes of patch antennas [19]

According to the studies conducted on comparing the performance of various antenna shapes, it has proven that the rectangular microstrip patch antenna shows better performance compared to circular and rectangular. The X-band frequency range which is from 8-12 GHz has allocated for radar applications by IEEE. Therefore, achieving a high directivity and gain is a main goal of devices that are used for these applications. The experiment done by R. Kiruthika and Dr. T. Shanmuganantham has confirmed that this goal can be achieved by rectangular patch antennas. A wider bandwidth can be achieved from circular patches. Triangular patch antennas have narrow bandwidth and low gain and directivity. As this research mainly focused on improving the gain and the directivity of the microstrip patch antenna it was decided to use rectangular shape for antenna patches [19].

As the beginning of the designing process, the single patch was simulated using probe feed method. The aim was to get an idea about the gain and the directivity of the patch antenna at 11 GHz.

4.1.2 probe feed technique

This method was used to check the gain and directivity of the patch without the effect of transmission lines radiation. The width and length of the patch antenna was calculated using 3.2 and 3.4. Initially the width and length was calculated as 10.77 mm and 8.128

mm respectively. Then the top of the ground plane and the bottom of the antenna was connected using a probe. As the port impedance of the network analyzer is 50, the probes impedance was set to the same value.

The design parameters of the antenna with probe feed has presented below 4.1.

Symbol	description	value (mm)
W	Width of the patch	8
L	Length of the patch	8.128
Wg	Width of the ground plane	2*L
Lg	Length of the ground plane	2*L
ht	Height of the ground plane	0.017
hs	Height of the substrate	1.575
f_p-y	Distance from the centre of the patch along y axis	2.7

Table 4.1: Parameters List of the Patch Antenna

After designing the patch according to above parameters 4.3, 4.4, the 50 Ω probe was located at the centre of the patch where the impedance is zero. Then the antenna was simulated by moving the probe location away from the centre. It was done by varying f_p-y parameter until the antenna's impedance matches with the probe feeds 50 Ω impedance. In addition the width and length of the patch antenna was swept to improve the impedance matching. It was found that the impedance matching is highly depending on the length of the antenna than its width.

The desired impedance matching could obtain at the point where the probe is 2.7 mm

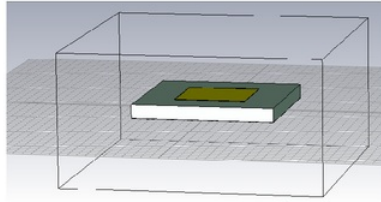


Figure 4.3: Patch Antenna Element

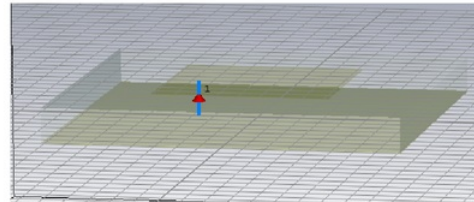


Figure 4.4: Probe Feed technique

away from the centre 4.5. Also the width of the antenna was tuned to 8 mm. This means that the most amount of the delivered power is received by the antenna and less amount of power is reflected back.

The simulation results of the antenna show that the directivity (ideal gain) is -12.9 dB at 11 GHz 4.6. The realized gain of the patch was found as 12.6 dB from its far-field pattern 4.7. The 3D and the Cartesian format of the radiation pattern prove that the side lobe level is very low for this ideal patch antenna.

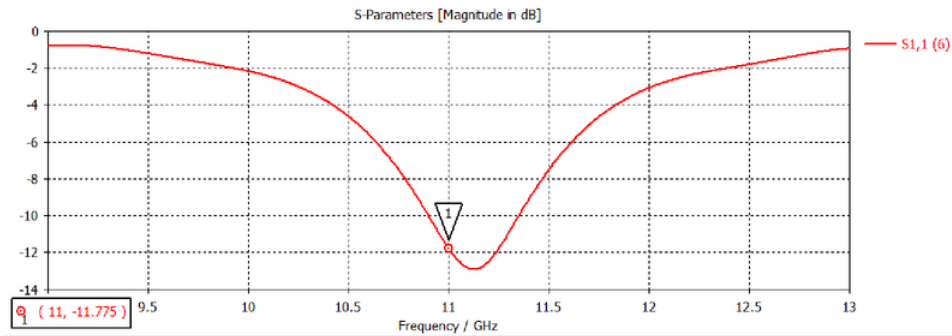


Figure 4.5: Reflection coefficient of single patch

Furthermore, the VSWR of the antenna was obtained as 1.696 at 11 GHz which is less

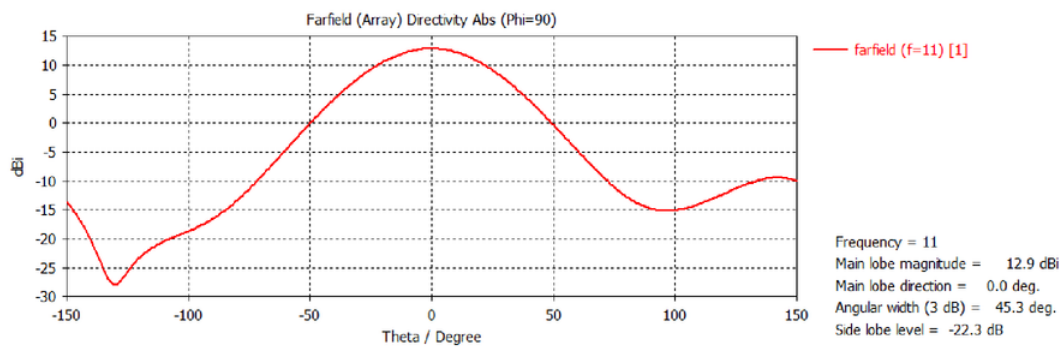


Figure 4.6: Radiation pattern in Cartesian plane

than 2 4.8. Therefore it can be conclude that the antenna has a good impedance matching at probes current location.

4.2 Far-Field Arrays

At the next stage, the above single element antenna was used to create far-field arrays. The aim was to get an idea about spacing between elements of antenna array to achieve a high gain and directivity at 11 GHz. It also aimed to investigate the radiation pattern of the antenna array with variations of element spacing.

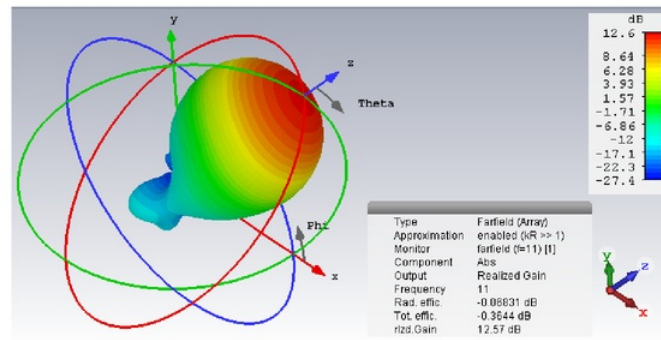


Figure 4.7: Radiation pattern in 3D plane

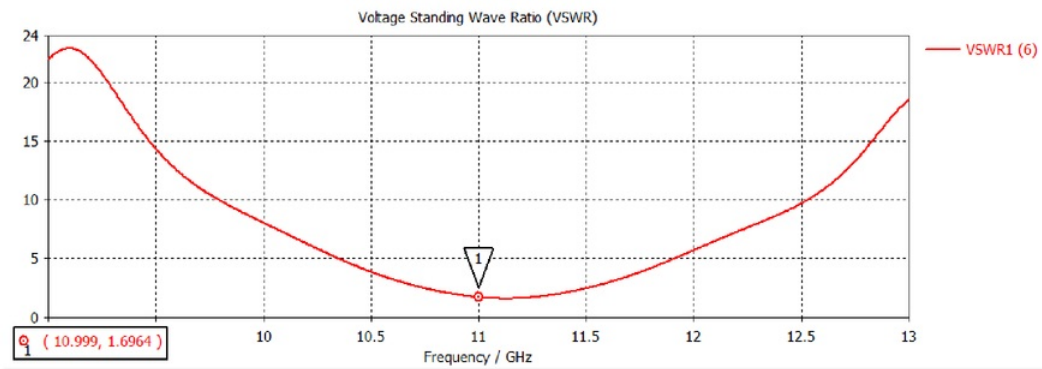


Figure 4.8: VSWR result for patch antenna

As mentioned before, this project only investigated about rectangular shape antenna arrays. At this stage element spacing was considered in terms of λ_0 . The table below presents the different antenna spacing and corresponding realized gains for three rectangular antenna arrays.

Antenna array	Spacing (mm)	Realized gain (dB)
4×4	$\lambda_0/2 = 13.5$	17.1
	$\lambda_0/4 = 6.75$	12.1
	$\lambda_0 = 27$	19.2
4×1	$\lambda_0/2 = 13.5$	12
	$\lambda_0/4 = 6.75$	9.53
	$\lambda_0 = 27$	13.5
3×3	$\lambda_0/2 = 13.5$	14.7
	$\lambda_0/4 = 6.75$	10.1
	$\lambda_0 = 27$	16.9

Although the 4×4 antenna array shows a high gain when the element spacing is λ_0 , its radiation pattern shows a high side lobe level 4.9. High side lobe levels means that the energy wastage is high which is not favourable for improving the directivity of the antenna. When the spacing is $\lambda_0/4$, the patch antennas start to overlap with each so it cannot be considered for designing purposes. When the spacing is $\lambda_0/2$, antenna has a gain of 17.1 dB at 11 GHz with low side lobe level at -15 dB 4.10. Also it shows a perfectly symmetrical radiation pattern 4.11.

Similarly, 4×1 rectangular antennas show high side lobe levels for λ_0 and $\lambda_0/4$ element

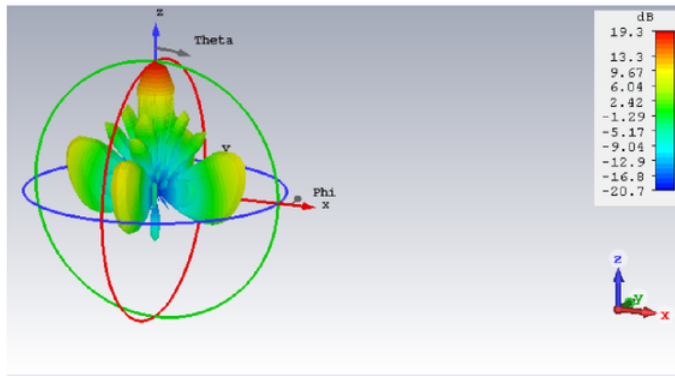


Figure 4.9: Gain of the 4×4 array for λ_0 element spacing

spacing 4.12. It also has a high gain and low side lobe levels when the spacing is $\lambda_0/2$ 4.13. However, it was noted that their side lobe level is less than the 4×4 antenna array and the radiation pattern was not symmetric.

The 3×3 antenna array shows a realized gain of 14.7 dB and low side lobe level when the elements are placed $\lambda_0/2$ distance apart 4.14. The Cartesian form of antenna array's radiation pattern proves that it has a symmetric radiation pattern. It also shows high side lobes when the element spacing are λ_0 . As before, the $\lambda_0/4$ spacing causes to overlapping

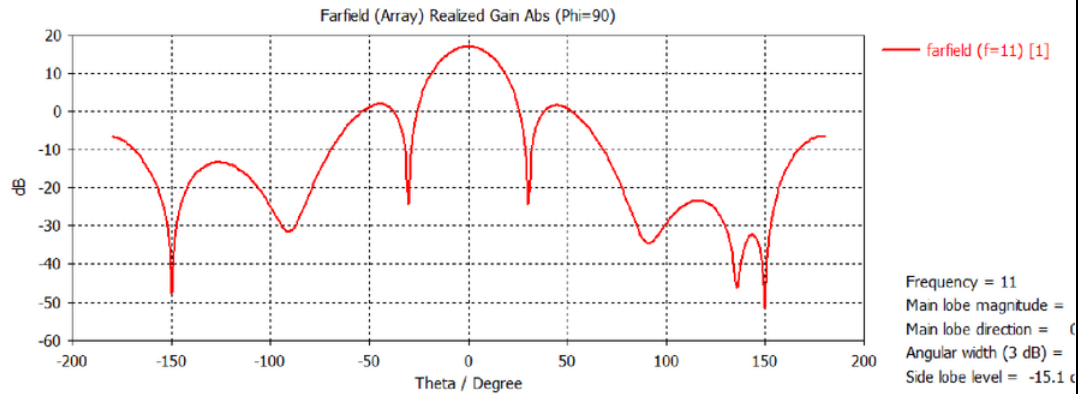


Figure 4.10: Radiation pattern of the 4×4 array for $\lambda_0/2$ spacing

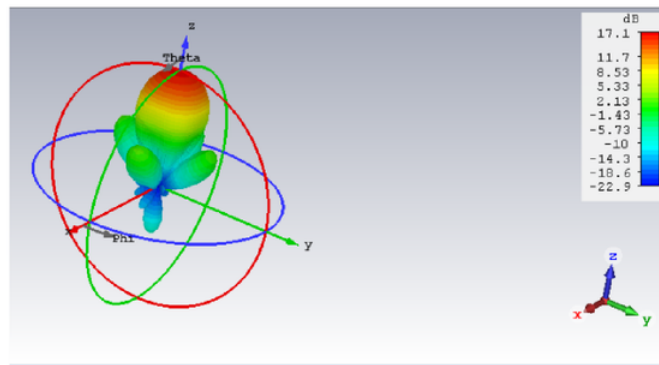


Figure 4.11: Symmetrical radiation pattern of the 4×4 array for $\lambda_0/2$ spacing

of the patches.

So, it was concluded that $\lambda_0/2$ is the most suitable element spacing for the antenna array in order to achieve a high gain and directivity. It could also notice that the radiation pattern is symmetrical for $\lambda_0/2$ element spacing only when the array is in square shape.

4.3 Ideal patch antenna array design

In the next stage, a 4×4 ideal antenna array was designed to examine the suitability of element spacing that was found using farfield arrays 4.15. The array was designed using

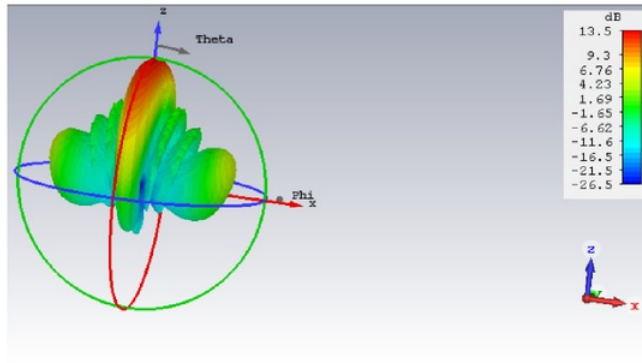


Figure 4.12: Radiation pattern of 4×1 array for λ_0 spacing

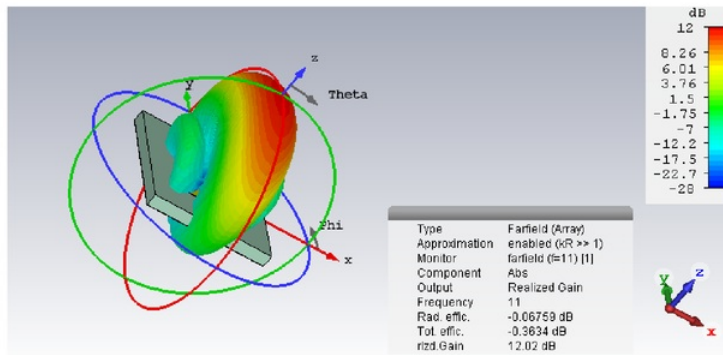


Figure 4.13: Radiation pattern of 4×1 array for $\lambda_0/2$ spacing

same patch antenna parameters with $\lambda_0/2$ element spacing. As this is an ideal array, a 50Ω probe feed was used for each antenna element instead of a feed network.

The simulation result shows that the antenna radiates in the broadside direction and has a realized gain of 18 dB [4.16]. This gain is bit greater than that of 4×4 farfield array with same element spacing. The side lobes of the radiation pattern are located 20 dB below the main. In addition, the radiation pattern of the ideal array was symmetric as expected.

Therefore $\lambda_0/2$, was considered as the most suitable element spacing for the antenna array at this stage.

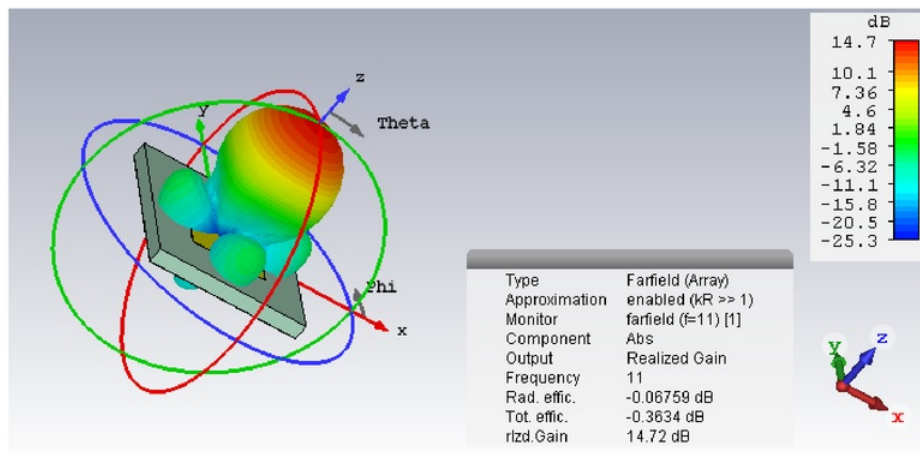


Figure 4.14: Radiation pattern of 3×3 array for $\lambda_0/2$ spacing

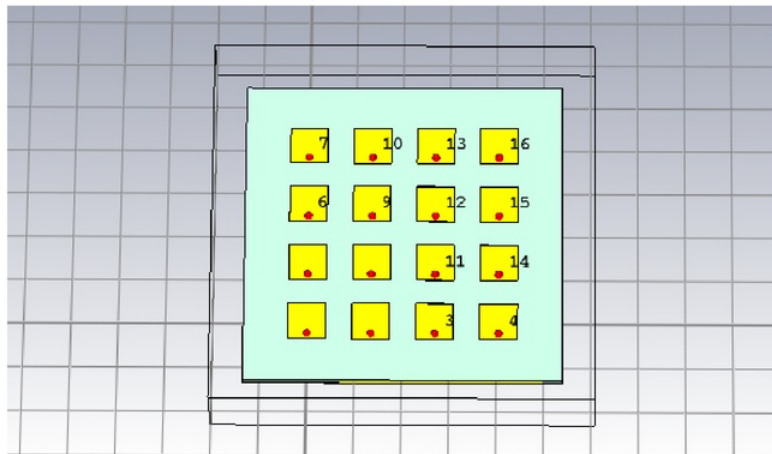


Figure 4.15: Ideal 4×4 patch antenna array

4.4 Feed network design

The feed network is the other main subsystem of an array, apart from patch antennas. In this stage of the project, some simple feed networks were designed to get an idea about how the dimensions of transmission lines affect to the impedance matching. Also it was aimed to get a better understanding of the behaviour of quarter wavelength transformers. Initially, it was decided to design a two way splitter which feed to two patch antennas.

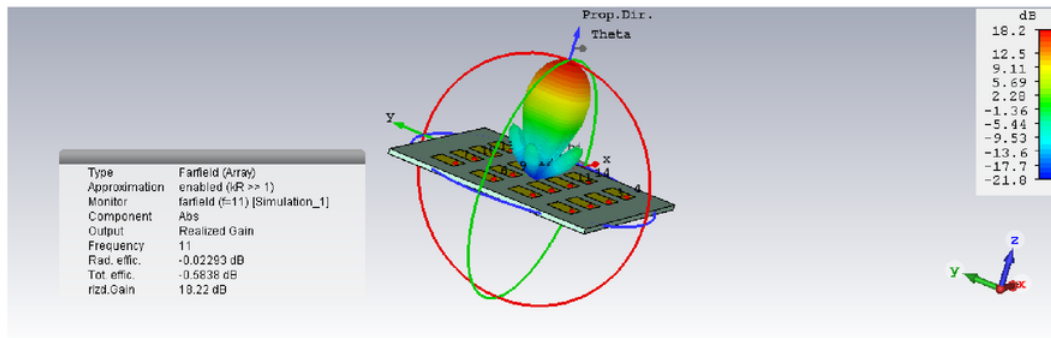


Figure 4.16: Radiation pattern of the ideal antenna array

4.4.1 Two Way Splitter feed network design 1

This two way splitter was designed using 50Ω , 100Ω transmission lines and two quarter wavelength transformers 4.17. It was assumed that the main 50Ω feed lines are connected to patch antennas. Two probes were located at the end of those feed lines to check impedance matching (probe 2 and 3). The horizontal transmission line was set to 100Ω such that it matches with the main 50Ω feed line at the centre of T junction. Therefore a quarter wavelength transformer was required to match the impedances between 100Ω transmission line and the 50Ω feed line that delivers power to patch antenna. The impedance of the quarter wave transformer was calculated using 3.6. Its length was set to $\lambda_0/4$ and width was calculated similar to a normal transmission line. The purpose of 50Ω bends was to reduce any mismatch between the quarter wavelength transformer and the 50Ω feed line. Then the feed network was simulated by varying width and length of the transmission lines. In this case, CST offers a parameter sweep function which is more efficient than manually changing the values. It allows users to select a range of values that a design parameter should be swept. It was found that the lengths of the transmission lines do not make significant difference to the simulation results. No changes were done to the length of the quarter wavelength transformers as its value is fixed by definition; But its width was varied in order to obtain desired impedance matching at 11 GHz.

The design parameters of the two way splitter has presented in 4.2.

A two way power splitter divide the input power equally to both patch antennas. The S21 and S31 represent the power delivered to each patch antenna. So, it was expected to get S21 and S31 approximately -3 dB as it represents half of power gain. The S11 should be less than -10 dB to have a good impedance matching. However the desired values for the S parameters were not achieved from the simulation results 4.18. The reflection

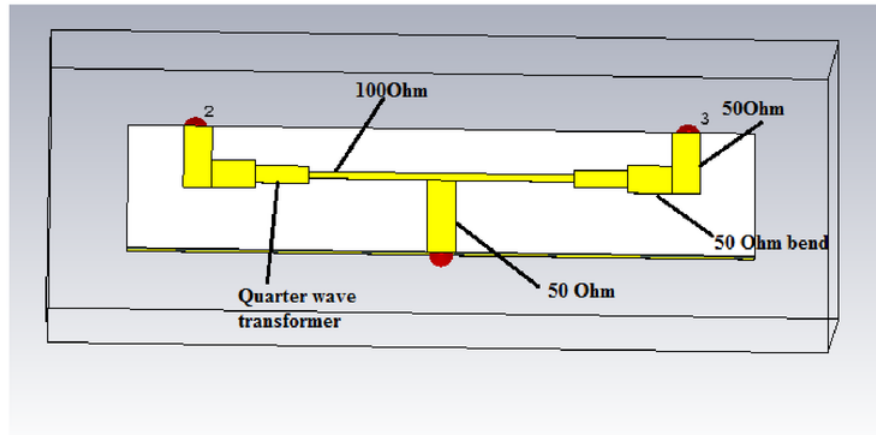


Figure 4.17: Two way splitter feed network 1

Symbol	description	value (mm)
Wa	Width of 50Ω feed lines	2.7
Wb	Width of 100Ω feed lines	0.7
La	Length of 50Ω feed lines	2
Lb	Length of 100Ω feed lines	10.284
WQ	Width of quarter wave transformer	1.7
LQ	Length of quarter wave transformer	5.0609
L_bend	Length of the bend	4.25

Table 4.2: Parameters List of Two Way Splitter Feed Network 1

coefficient was around -8.42 dB and S_{21}/S_{31} were -7.62 dB at the operating frequency. In the smith chart, it can be clearly seen that the impedance at 11 GHz is not 50Ω which proves that antennas is not impedance matched 4.20.

The farfield pattern shows that this feed network does not radiates in the broadside direction which can affect to the directivity of the entire antenna array 4.19.

So it was concluded that this two way splitter is not applicable for designing the feed network for actual antenna array.

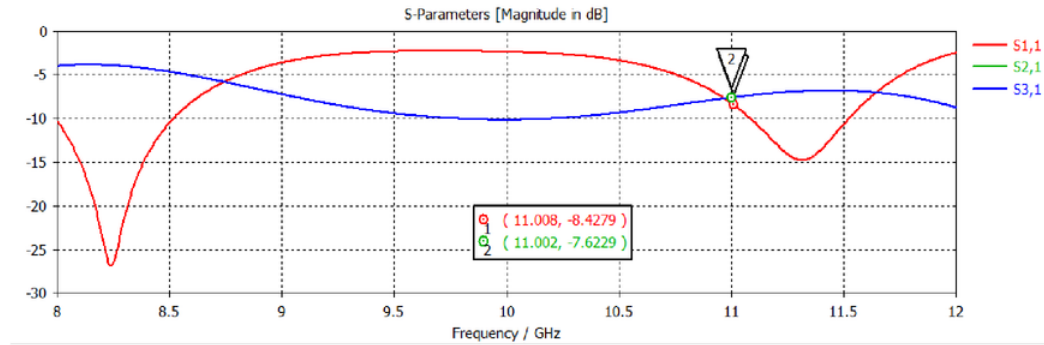


Figure 4.18: S parameters of the Two way splitter 1

4.4.2 Two Way Splitter Feed network design 2

The second two way splitter aimed to minimize the radiation of the feed network and to improve the impedance matching. The width of the 50Ω feed line is considerable larger compared to the dimensions of the patch antennas. So these transmission lines may radiate significantly affecting the radiation pattern of the patches. If the impedances of the transmission lines are reduced, their width also reduces leading to a low amount of radiation due to feed network. As it is expected to minimize the radiation of the feed network, the impedances of transmission lines were selected as 100Ω and 200Ω . This two way splitter uses an additional quarter wave transformer at the input to match the impedance of 50Ω input probe and the 100Ω transmission line.

The design parameters of the feed network has given in 4.3

Symbol	description	value (mm)
Wa	Width of 100Ω feed lines	1.4116
Wb	Width of 200Ω feed lines	0.1674
La	Length of 100Ω feed lines	5
Lb	Length of 200Ω feed lines	8
WQ100	Width of quarter wave transformer (100Ω to 50Ω)	2.78
LQ100	Length of quarter wave transformer (100Ω to 50Ω)	5.06
WQ200	Width of quarter wave transformer(200Ω to 50Ω)	2.78
LQ200	Length of quarter wave transformer(200Ω to 50Ω)	5.06

Table 4.3: Parameters List of Two Way Splitter Feed Network 2

Although the design parameters were swept to detect an impedance matching the results it couldn't be achieved. Also the feed network was not radiating in the broadside

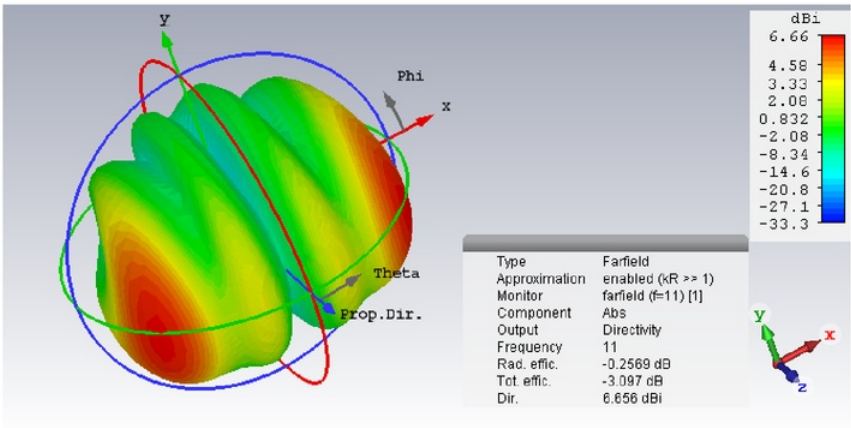


Figure 4.19: 3D Radiation pattern

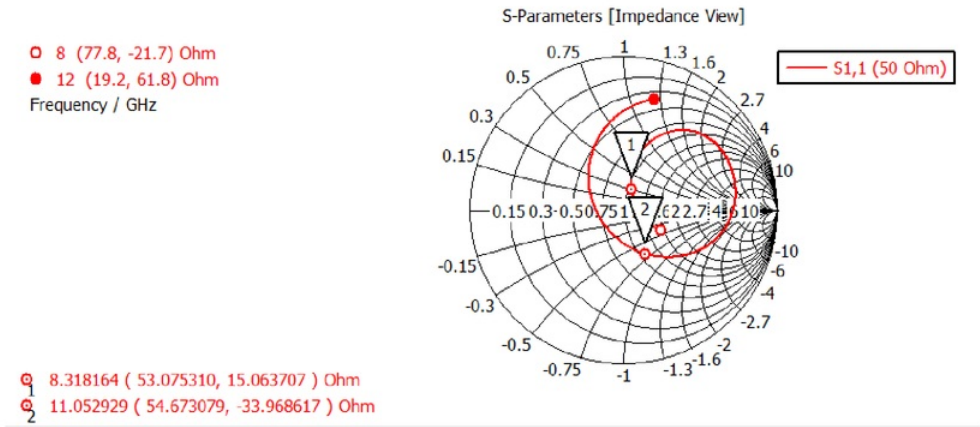


Figure 4.20: Smith chart

direction 4.22.

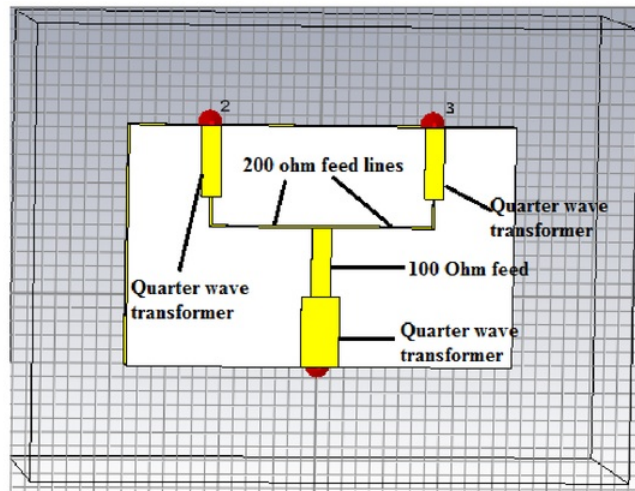


Figure 4.21: Two Way Splitter Feed Network 2

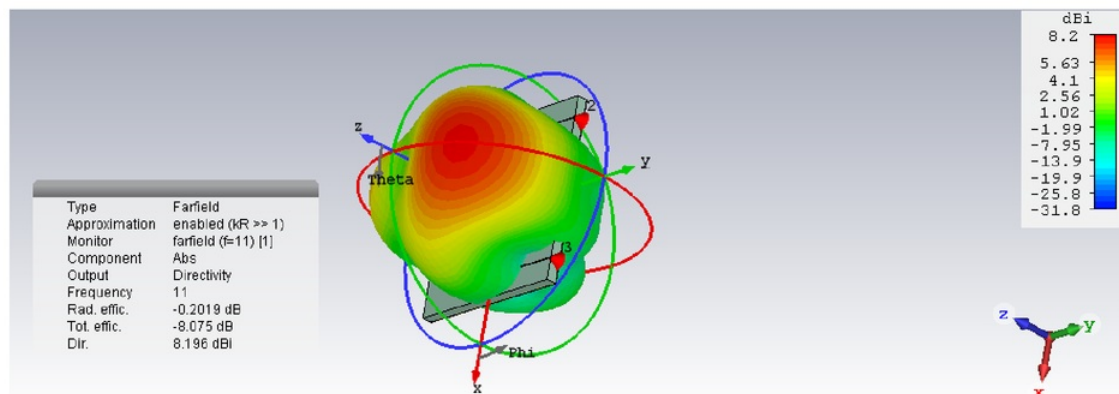


Figure 4.22: Radiation pattern of the two way splitter feed network 2

Chapter 5

Development of Patch Antenna Array

Previously, the two way splitters were designed by considering arbitrary values for the edge impedances of patch antennas without actually designing them. As explained in the previous chapter, it was not be able to achieve the desired impedance matching for those two way splitters. Therefore it was decided to implement the feed networks with actual edge impedances of antenna patches. The impedances of the transmission lines were selected as 100Ω and 200Ω to reduce the radiation due to feed network. The lengths of all the quarter wave length transformers were initially considered as $\lambda_g/4$ instead of $\lambda_g/4$ to improve the accuracy. The arrays were designed on same substrate (RT5880) that has a height of 1.575 mm. The 4×4 array was designed in 5 stages which will be explained though out this chapter.

5.1 Single patch antenna with an edge feed

The first stage of the array designing was to implement a quarter wavelength transformer which matches the edge impedance of the patch antenna and the 200Ω transmission line 5.1. For now, a 200Ω discrete port was connected at the end of the quarter wave transformer to represent the impedance of the transmission line. It is important to locate the discrete port at the centre of edge line of the transformer. Otherwise, the transformer may not recognize 200Ω impedance at the input which can affect the simulation results. It could be identified that the simulation results can vary slightly depending on the location of the discrete port. Better results were archived when it was placed at the centre of the input of quarter wavelength transformer.

The edge impedance of the patch antenna with 8×8.128 mm dimensions was found as 254.91Ω . It should be noted that all the calculations are done by considering 11 GHz as the operating frequency. The width of the quarter wavelength transformer was calculated similar to a normal transmission line. The length was considered as $\lambda_g/4$ as explained in

before.

After implementing the initial design, the length of both patch antenna and the quarter wavelength transformer was tuned to get a good impedance matching at 11 GHz. The optimised length of the patch antenna was 7.8 mm and the width was kept constant

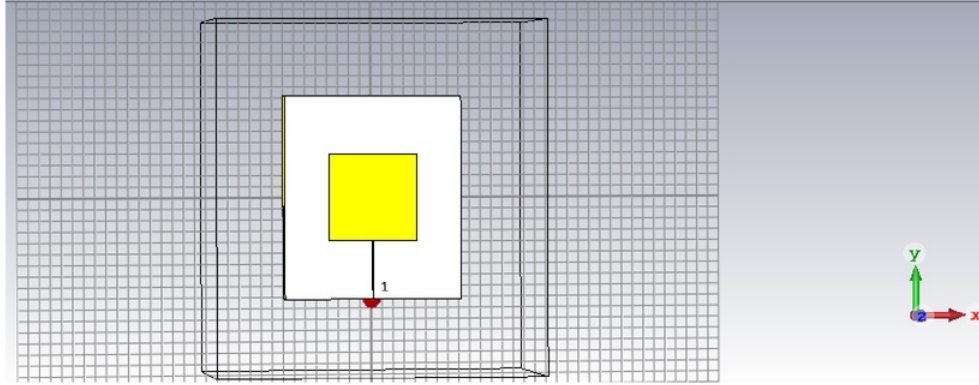


Figure 5.1: Single patch antenna with quarter wavelength transformer

5.1.1 simulation Results

The reflection coefficient S_{11} of the patch antenna has a minimum value of -17.12 dB at 11 GHz which proves that most of the input power is received by the antenna 5.2. However it doesn't mean that all the received power will be radiated. It can be radiated or can be absorbed by the antenna as internal losses. Also its VSWR was 1.32 which is less than 2 5.3. Therefore it was concluded that the patch antenna was impedance matched at its operating frequency as expected.

The realized gain of the patch antenna is 12.7 dB and has very low side lobe level at -22.3 dB 5.4. Although the radiation pattern is not perfectly symmetric, it does not show a significant difference. The 3 dB angular width of the single patch antenna is 45.3 degree which is quite high. If the angular width is reduced the main lobe becomes more focused such that the antenna can achieve a high directivity. Therefore one of the aims of designing an antenna array is to improve the directivity by reducing this angular width.

In addition, the 3D radiation pattern 5.5 shows that the patch radiates in the broadside direction where $\Theta/\phi = 0$.

As explained before, the electromagnetic field of a radiating antenna consists of an E-field component and a H field component. According tangential E-field pattern 5.6, it can

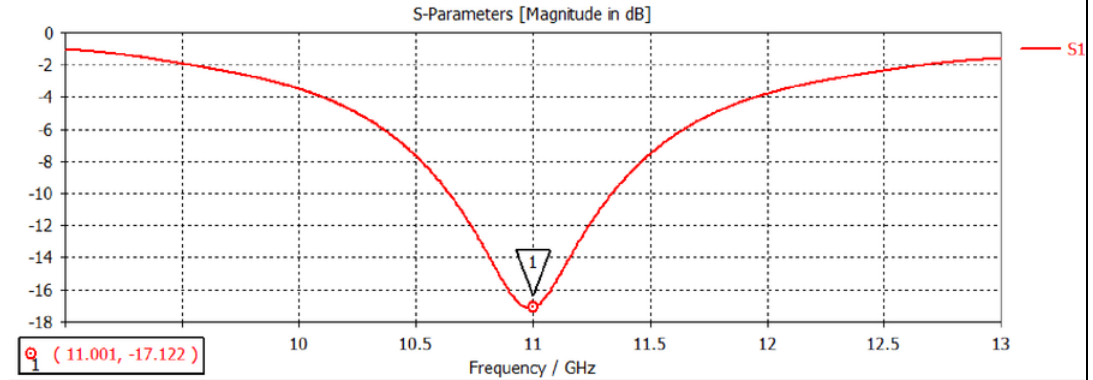


Figure 5.2: Reflection coefficient (S11) of patch antenna

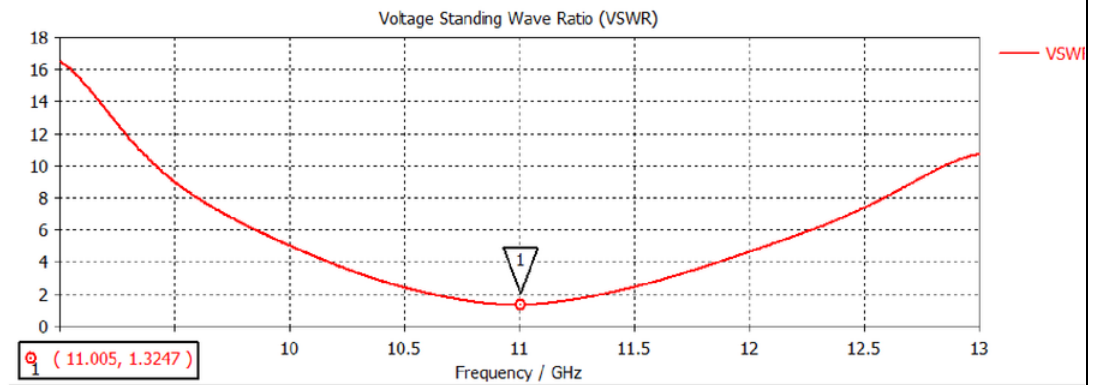


Figure 5.3: VSWR simulation results

be clearly identified that the E field is strongest along the two edges where the signal is fed and the edge directly opposite to the feeding edge; which means that the e-field moves vertically back and forth from feeding edge to its opposite edge. Therefore, the antenna can be identified as a linearly polarized antenna. These edges of the patch antenna are commonly called as radiating edges. In addition, fewer amount of e-field lines can be seen in the other two edges of the patch.

The patch antenna has a strong E-field along its length. Therefore, it should be noted that the length is the critical factor when tuning the patch to operate at a desired frequency.

The x and y components of the E-field also prove that the antenna mainly radiates in the vertical direction. According to the results, the e-field is stronger in the vertical plane

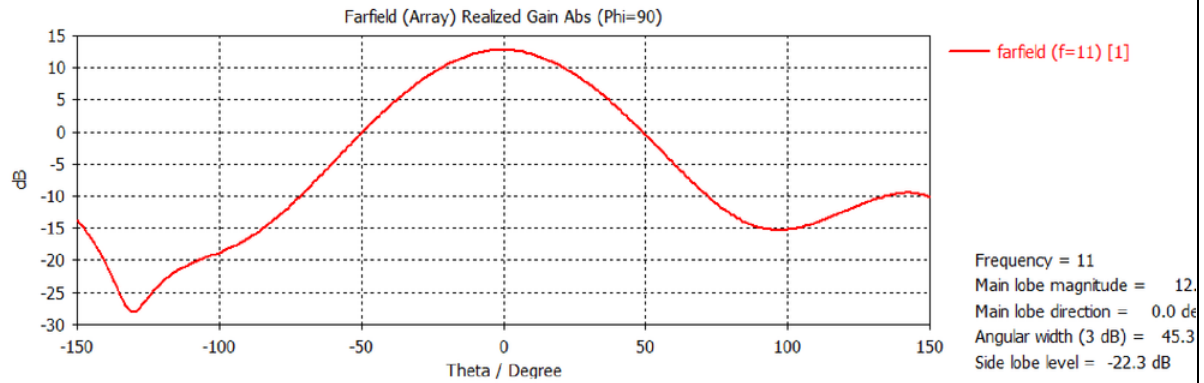


Figure 5.4: Radiation patten in Cartesian plan

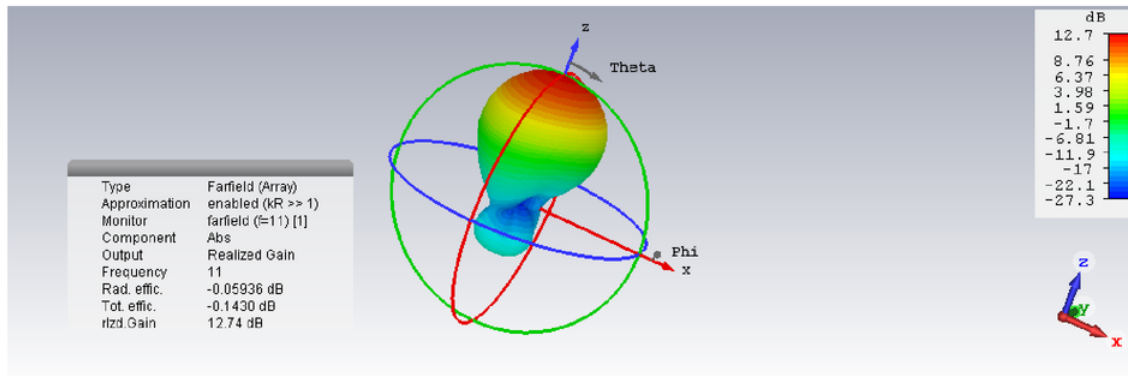


Figure 5.5: 3D radiation patten of the antenna

(y)5.8 than in the horizontal plane(x) 5.7. This means that the E-field mainly consists of E_y field such that E_x is negligible. Therefore the antenna satisfies the requirement of radiating in the broadside direction.

According to the basic EM theories, the h-field is always perpendicular to the e-field. It can be clearly seen that the directions of field indicating arrows in 5.9 and 5.1 are perpendicular to each other.

This patch antenna and the quarter wavelength transformer were used in the next stage of the designing process to implement 2×1 array.

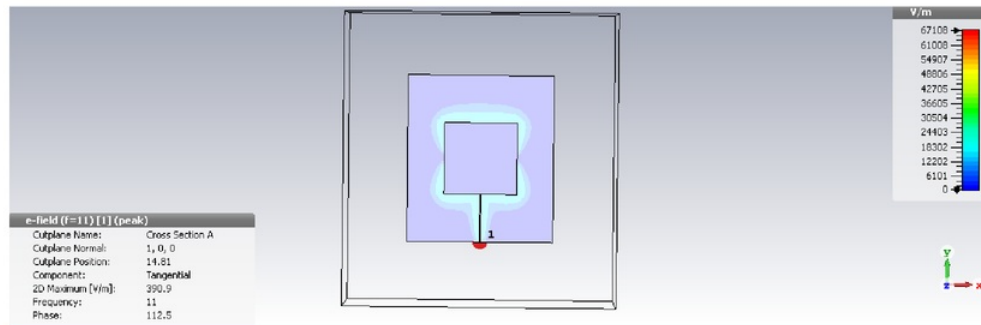
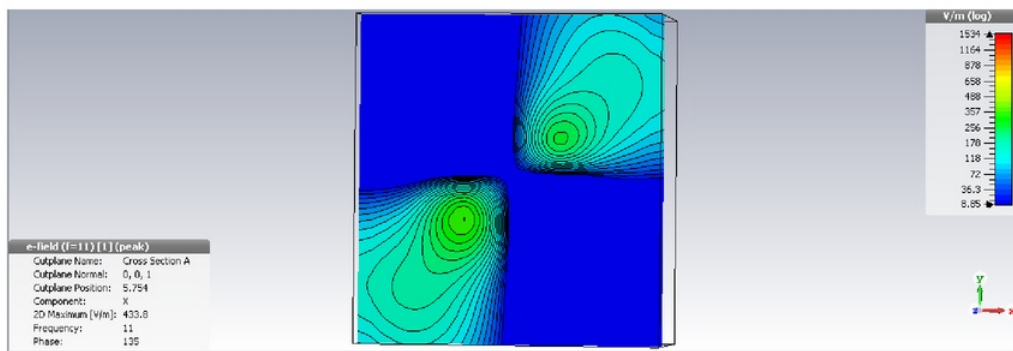
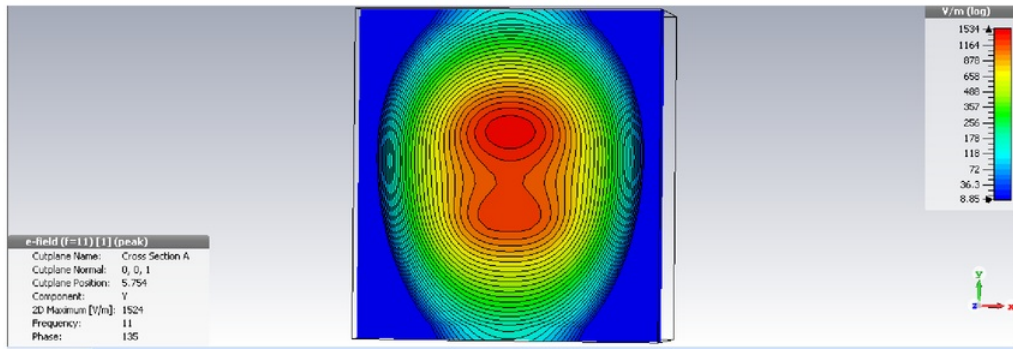


Figure 5.6: Tangential E-field pattern

Figure 5.7: E_x component of the E-fieldFigure 5.8: E_y component of the E-field

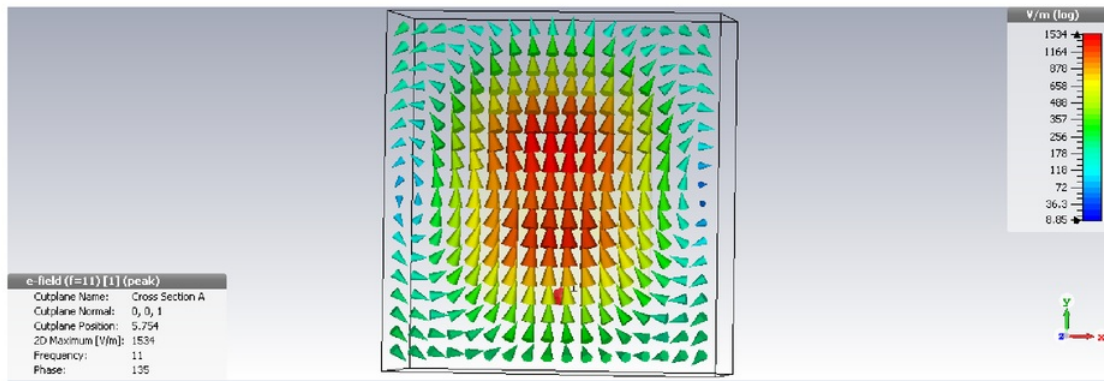


Figure 5.9: Direction of E-field

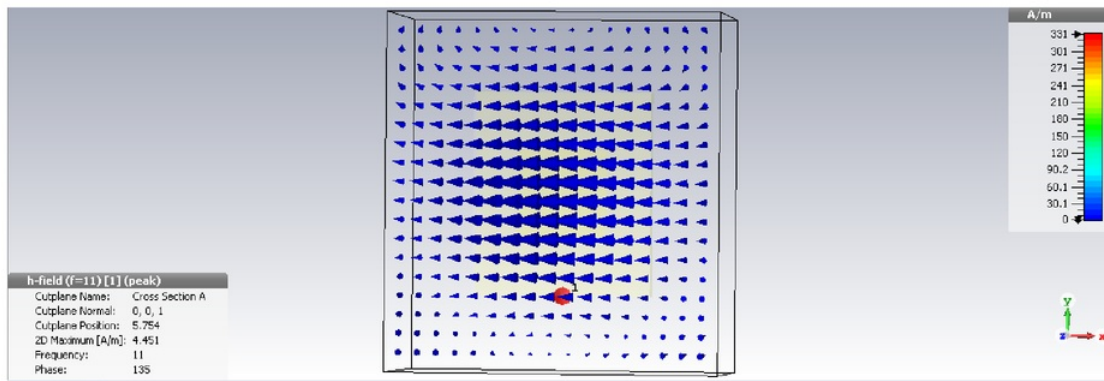


Figure 5.10: Direction of h-field

5.2 The 2×1 array design

In this stage of the project a 2×1 array was designed using the previous single patch. Here, each quarter wavelength transformer which is used to match the impedance of the patch antenna is connected with an actual 200Ω feed line. It was decided to use more amount of 200Ω feed lines than 100Ω feed lines for the feed network. It aims to further reduce the effect of the radiation due to feed network. The centre of the T junction has an impedance of 100Ω . Therefore, another transformer was used to match 100Ω with 200Ω impedance such that a 200Ω feed line can be used when designing the 2×2 array. For the simulation purposes, the 200Ω discrete port was connected at the input to represent a 200Ω feed line. The spacing between the elements is critical factor when designing an

antenna array. In this design, the 200Ω horizontal feedline controls the spacing between two patch antennas. Initially the spacing between antenna elements was set to $\lambda_0/2$ as found by investigating Farfield arrays. So the total length of 200Ω horizontal feedline was set to 13.5 mm ($\lambda_0/2$).

In addition, the basic design parameters such as heights of the substrate, ground plane and patch were kept constant.

After designing the 3D model 5.11 of the array it was optimized by tuning design parameters. These parameters were varied using parameter sweep function in order to obtain a high gain and impedance matching at 11 GHz.

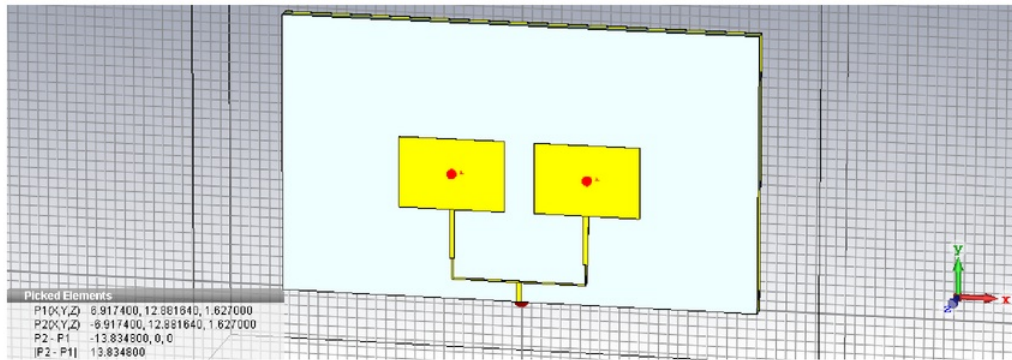


Figure 5.11: 3D model of the array

Basically, the length and width of both patch antennas and quarter wavelength transformers were tuned to get the impedance matching at the resonant frequency. Especially the dimensions of the patches were adjusted slightly than that of single patch antenna design. The width of the patch was increased to 10.78 mm and length was reduced to 7.3 mm. The initial spacing was not required to change at this point.

5.2.1 simulation results

After tuning the design parameters, the reflection coefficient was obtained as -16.157 at 11 GHz. Although this is not the minimum value of the S11 graph, it satisfies the requirement of been less than -10 dB 5.12. So it proves that the amount of power reflected back by the antenna is negligible. The VSWR of this antenna array at 11 GHz is 1.37 which is expected from a well impedance matched antenna design 5.13.

The 3D radiation pattern of the 2×1 antenna array confirms that the antenna has a directivity of 9.49 dBi and a realized gain of 9.37 dBi 5.14. The realized gain is less than

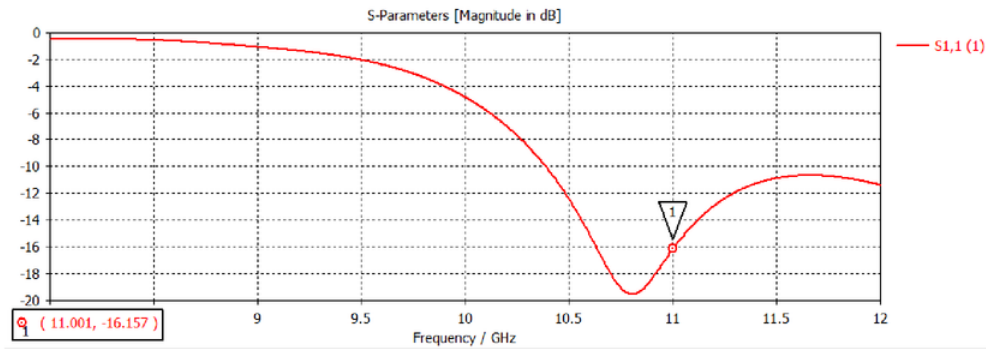
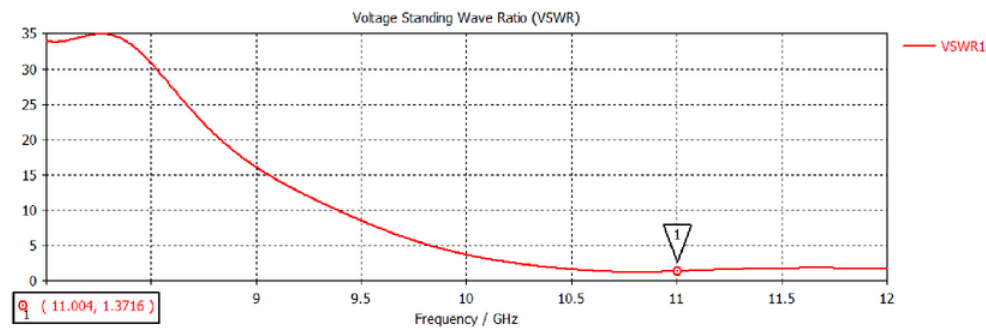
Figure 5.12: Reflection coefficient(S_{11})

Figure 5.13: VSWR of the antenna array

the directivity as it considers the actual losses that occurred while radiating EM waves. In an actual situation this difference can be quite high.

The polar and Cartesian forms 5.15 of the radiation pattern show that the direction of main lobe has shifted 12.0 deg from the broadside direction. At this stage of the design this 12.0 deg shift was negligible.

Similarly the E field and H field components of the array can be plotted using Farfield monitor.

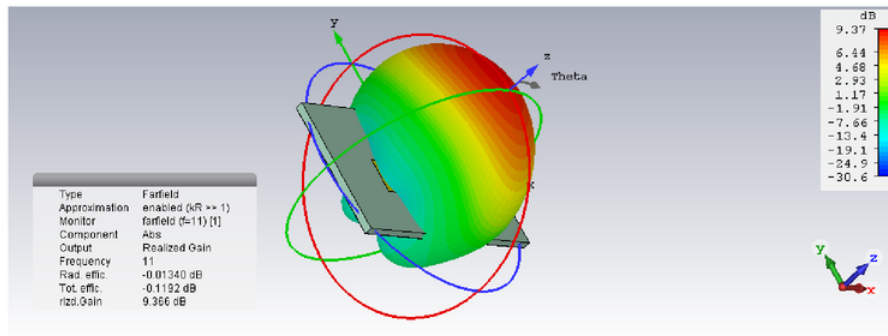


Figure 5.14: 3D radiation pattern of the array

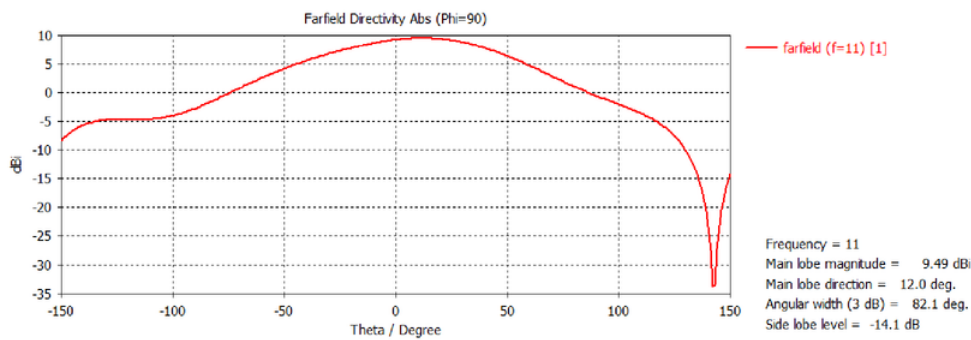


Figure 5.15: Cartesian form of the radiation pattern

5.3 The 2×2 array design

The 2×2 array was implemented using previously designed 2×1 array 5.17. It was transformed along the Y axis and obtained a copy of the original array at a desired distance. It should be noted that the array cannot be copied using mirroring function of CST as it will create an upside down copy of the original array 5.16. If an upside down copy was used to design 2×2 array it will lead to a 180 degree phase shift in the radiation pattern. More importantly, the impedance matching could not be achieved for such array.

The 200Ω discrete port in previous design which was used to represent 200Ω transmission line was removed. Then the original array and the transformed array were connected using a 200Ω transmission line. It allows to change the vertical spacing between patch antennas as required. In addition the quarter wave transformer of the transformed array was moved upward to make it easier to connect the transmission line. Then a quarter wavelength transformer was designed at the centre of this 200Ω feed line to transform 100Ω impedance

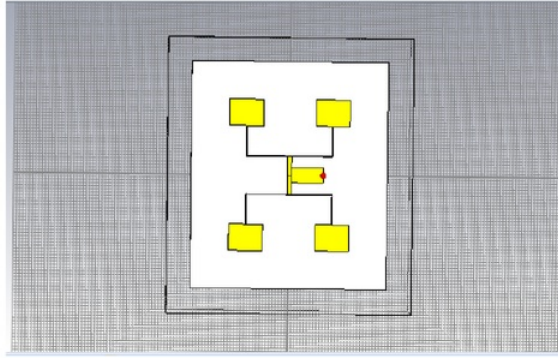


Figure 5.16: The array designed by mirroring 2×1 array

to 200Ω . The other end of this quarter wave was connected to a 200Ω transmission line and input was supplied through a discrete port.

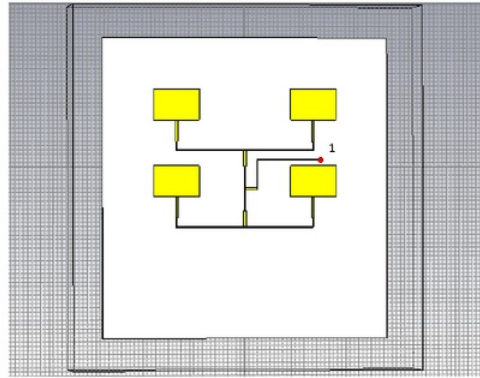


Figure 5.17: The finalized 3D model of the 2×2 array

In this stage of the antenna array, the length of each quarter wavelength transformer at the T junction was set to $\lambda_g/4$. The aim was to improve the accuracy of the design parameters. Then the vertical and horizontal spacing between patches were tuned in order to achieve impedance matching at 11 GHz. Also, the widths and lengths of the quarter wave length transformers were slightly varied. The parameter sweep function of CST is very efficient when it is required to vary more than one parameter at the same time. In addition the size of the patch antennas was not required to be changed.

5.3.1 Simulation results

The array was impedance matched when its horizontal and vertical spacing between antenna elements were tuned to $1.7\lambda_g$ and λ_g respectively. The reflection coefficient of the array was obtained as -21.7 at 11 GHz 5.18. Also its VSWR was less than 2 which indicates that the array is impedance matched at the operating frequency 5.19. According

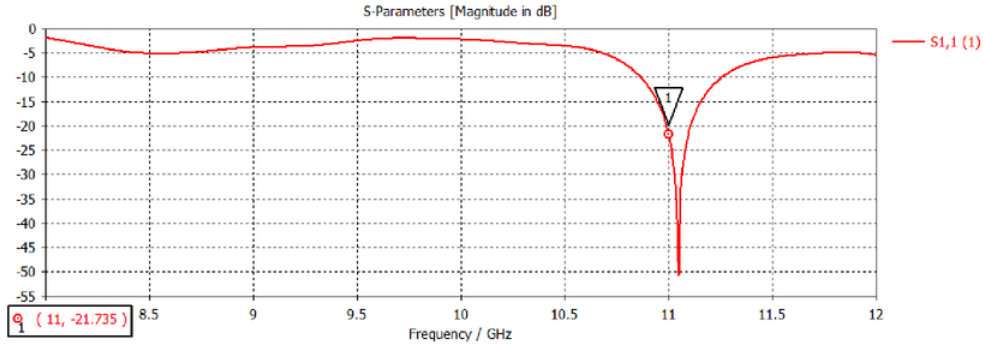


Figure 5.18: Reflection coefficient(S11)

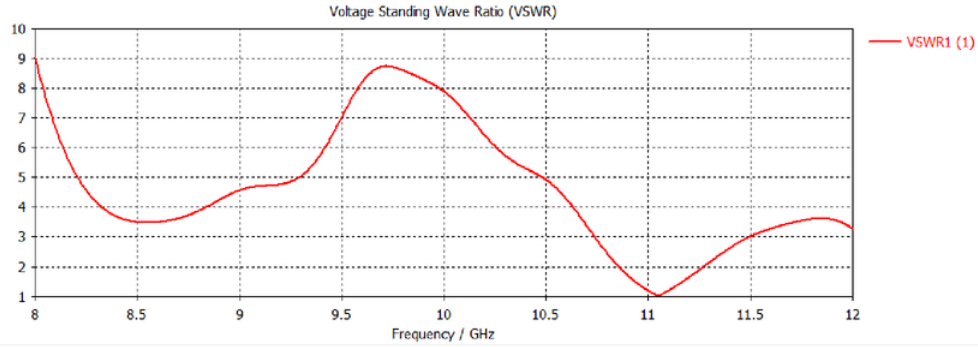


Figure 5.19: VSWR of the antenna array

to the Cartesian form 5.20 of the radiation pattern, the antenna array has a directivity of 13 dBi at its resonant frequency. Also it radiates in the broadside direction and has a realized gain of 12.9 dBi 5.21. In addition, the main lobe of the radiation pattern has skewed 1 degree off $\Theta = 0$ which is negligible at this stage. However the radiation pattern of the array is reasonably symmetric along the broadside direction.

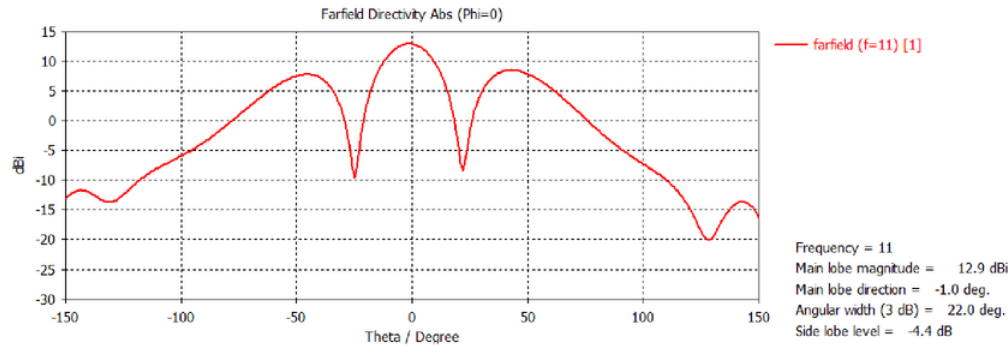


Figure 5.20: Cartesian form of the radiation pattern

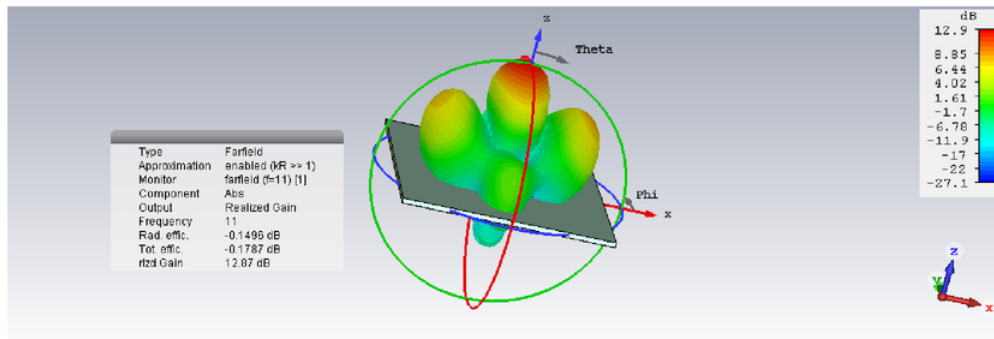


Figure 5.21: 3D radiation pattern of the array

5.4 The 2×4 array design

This array consists of 8 micro-strip patch antennas 5.22. It was implemented by mirroring the 2×2 antenna array along y-axis. The 200Ω transmission line of 2×2 array which was used to connect the discrete port was extended to combine the two arrays. The length of this line controls the horizontal distance between these two arrays. Then at the centre of this line a quarter wavelength transformer was designed in order to match its centre impedance with the impedance of 200Ω transmission line. In the similar way, this additional 200Ω transmission line was used to connect a discrete port to supply the input power.

After designing the initial 3D model of the array, its physical parameters were tuned to achieve the impedance matching at 11 GHz. Similar to previous stage the, only the horizontal distance and the width of the last quarter wavelength transformer had to be tuned to get the impedance matching. The horizontal distance between the two arrays was

tuned such that the distance between two antenna elements is $1.7\lambda_g$. The vertical distance of λ_g was not required to tune at this point. The importance of tuning the arrays at each stage, is that it reduces the complexity of achieving the impedance matching at the final stage. It allows to obtain the matching by varying fewer amount of design parameters.

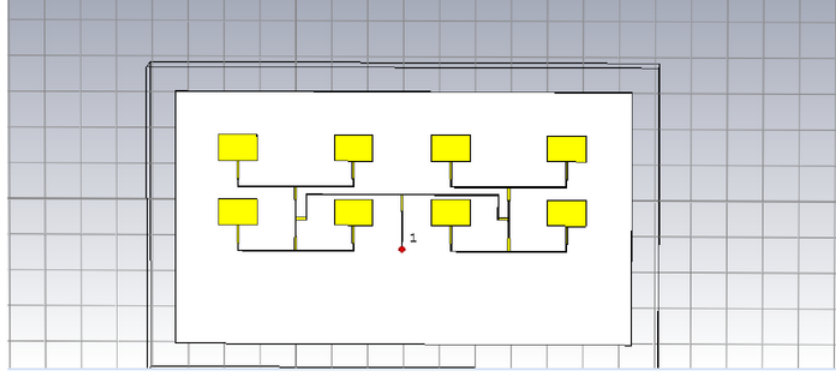


Figure 5.22: Finalized 3D model of the array

5.4.1 Simulation results

The antenna array has a reflection coefficient of -20 due to the spike close to 11 GHz 5.23. Its VSWR at operating frequency is less than two as expected 5.24. These results prove that this antenna array has an impedance matching at 11 GHz.

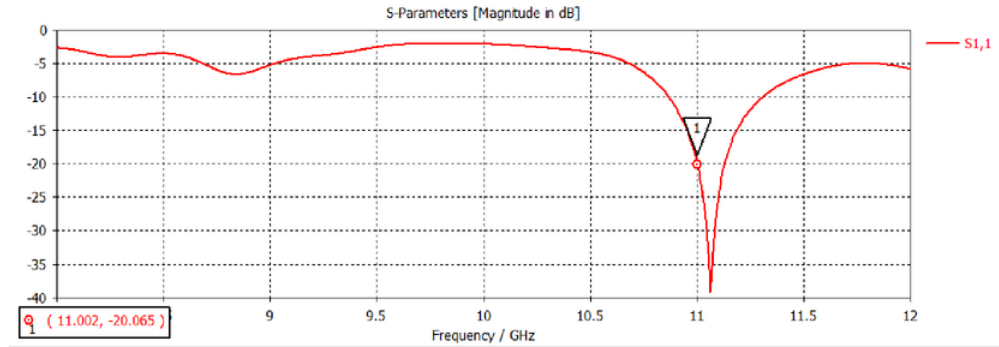


Figure 5.23: Reflection coefficient at 11 GHz

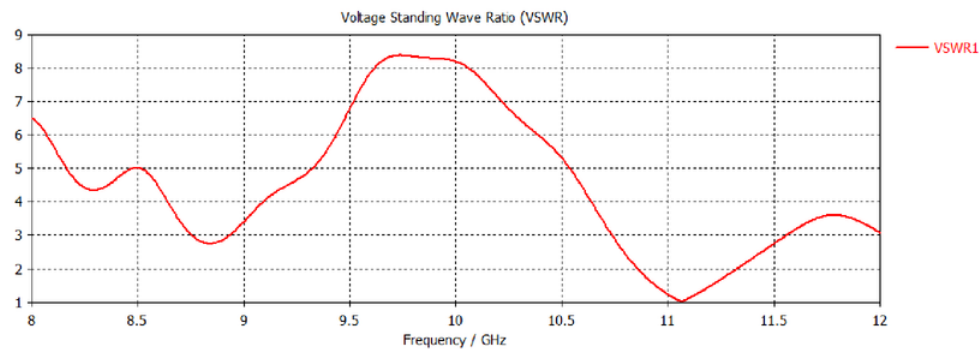


Figure 5.24: VSWR of the array at 11 GHz

According to the Cartesian form of the radiation pattern, the antenna array has a directivity of 15.4 dBi and side lobe level of -7.3 dB [5.25]. Its realized gain 15.1 dB is slightly less than the directivity as it considers the internal losses [5.26]. The 3D radiation pattern shows that the array radiates in the broadside direction as required.

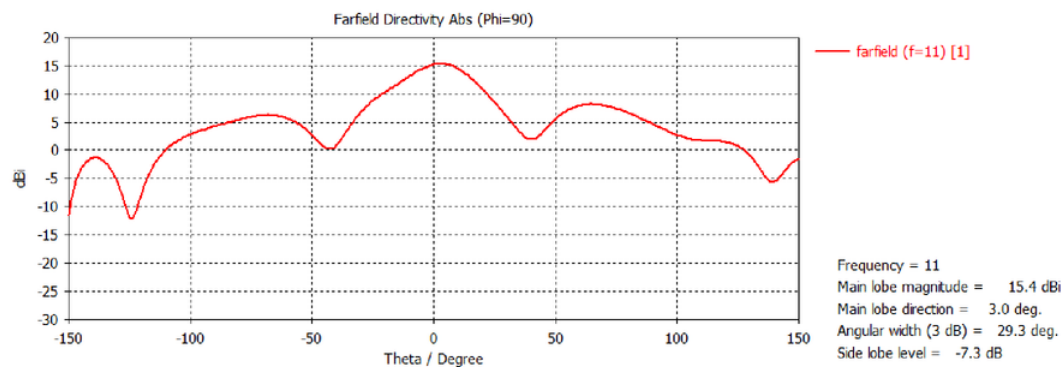


Figure 5.25: Directivity of the antenna array

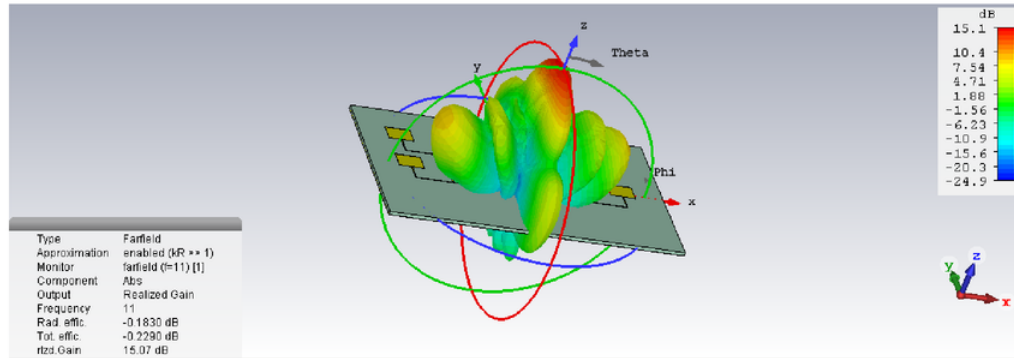


Figure 5.26: Realized gain of the array

5.5 The 4×4 array design

This is the final stage of the 4×4 patch antenna array design. Similar to previous stages, it was implemented by transforming 2×4 array along y axis. The two arrays were then connected by extending the 200Ω transmission line which was at the feeding end of the 2×4 array. This line was used to adjust the vertical distance between the two 2×4 arrays. A quarter wavelength transformer was designed at the middle of this transmission line to match its centre impedance of 100Ω with the 200Ω line which has used to connect the discrete port. The port impedance has set to 200Ω .

After implementing the initial antenna array, its design parameters had to be tuned in order to achieve the impedance matching at 11 GHz. As each sub array was tuned in previous stages, the final design required only few parameters to be tuned. The width of the last transformer, vertical distance between the 2×4 arrays and the length of the last 200Ω feed line was varied using CST optimizer tools. Any other parameters were not changed to get the impedance matching.

The vertical and horizontal distances between antenna elements has shown in 5.27. As this array was designed by combining four 2×2 arrays, the spacing between certain antenna elements is not same. The width and the length of each patch antenna are 10.78 mm and 7.3 mm respectively. The size of the entire antenna array is $125\text{mm} \times 101\text{mm}$.

5.5.1 Simulation results

When the antenna array was simulated with tuned design parameters, the S11 measurement was obtained as in 5.28. It clearly indicates that the power reflected back by the array is significantly low at the resonant frequency of 11 GHz. The reflection coefficient

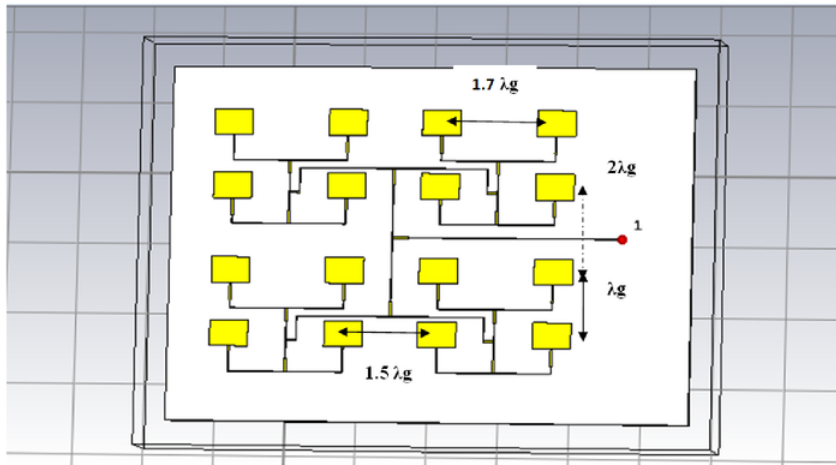


Figure 5.27: The 3D model of the 2×2 array and element spacing

of the antenna array can be obtained as -44.58 for the above frequency.

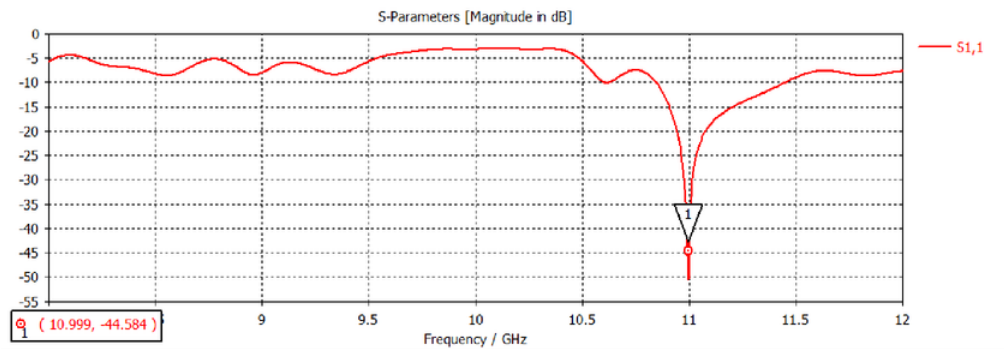


Figure 5.28: Reflection coefficient (S_{11}) of the array 11 GHz

The voltage standing wave ratio of the array is zero and satisfies the requirement of been less than 2 5.29. According to the real and imaginary parts of the impedance, the 11 GHz is the only frequency where the real part is 200Ω and the imaginary part is 0 5.30 5.31. This means that the antenna array is perfectly matched with the 200Ω input impedance.

The farfield pattern shows that the antenna array has a directivity of 18.4 dBi and

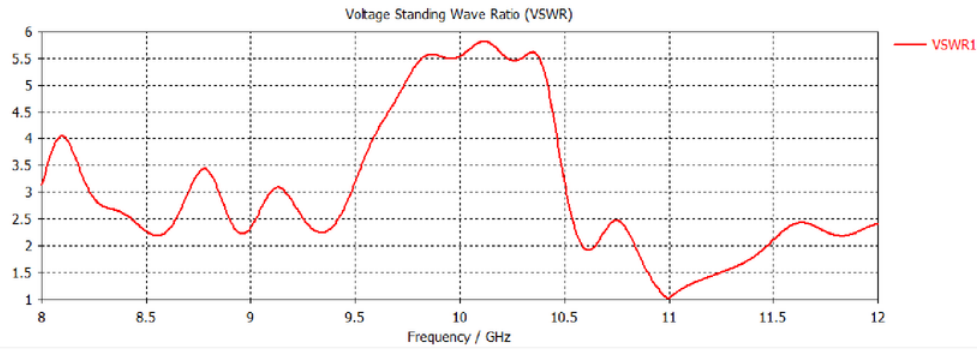


Figure 5.29: The voltage standing wave ratio (VSWR) of the array

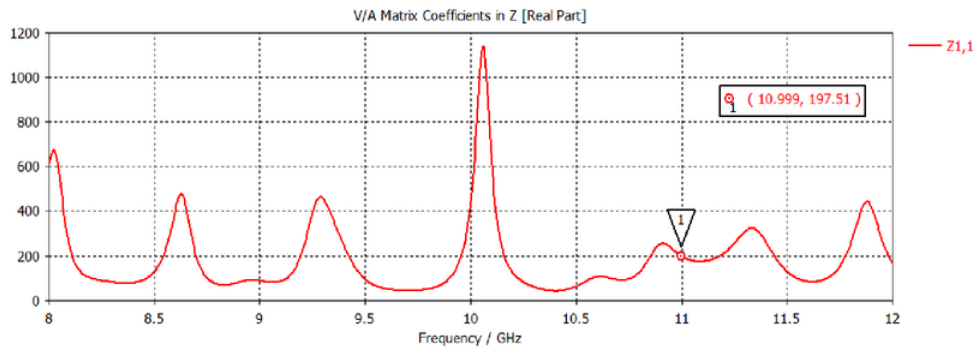


Figure 5.30: Real impedance of the array at 11 GHz

17.8 dBi realized gain in the broadside direction 5.32 5.33. This directivity and the gain of the 4×4 array is greater than that all the other sub arrays designed in previous stages. From this result it can be concluded that when the number of antenna elements increases the gain of the array increases. Therefore, a high gain and directivity can be achieved by increasing the number of patch antennas in an array.

According to concepts of antenna theory, the gain of an array can be expressed in terms of the gain of a single patch antenna (G_0) with same dimensions. For an array with two patches, it is given by $G_0 + 3$ dB. Similarly the gain of an array with 4 antenna elements is $G_0 + 6$ dB. Likewise, the gain of a 4×4 antenna array is expected to be $G_0 + 12$ dB. In this case the gain of the single patch is 12.7 dB. So the gain of the antenna array should be around 24.7 dB. But the simulation results only provide a gain of 18.4 dB which is less than the expected value. This happens due to the power wastage in the side

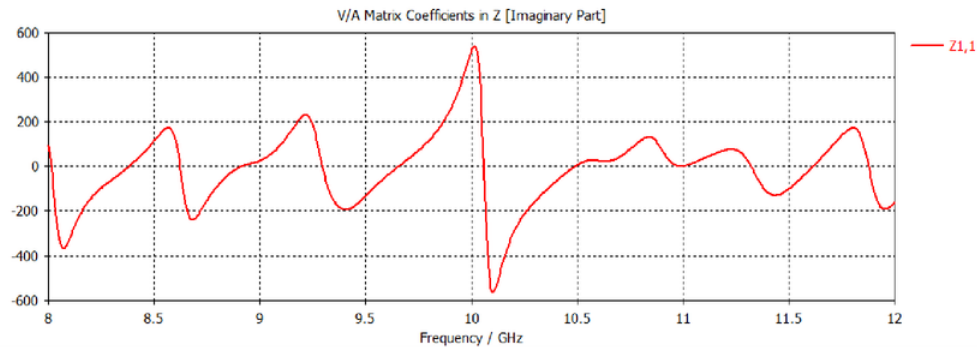


Figure 5.31: Imaginary impedance of the array at 11 GHz

lobes of the radiation pattern. Therefore the gain and the directivity of the array can be increased if the side lobes are reduced.

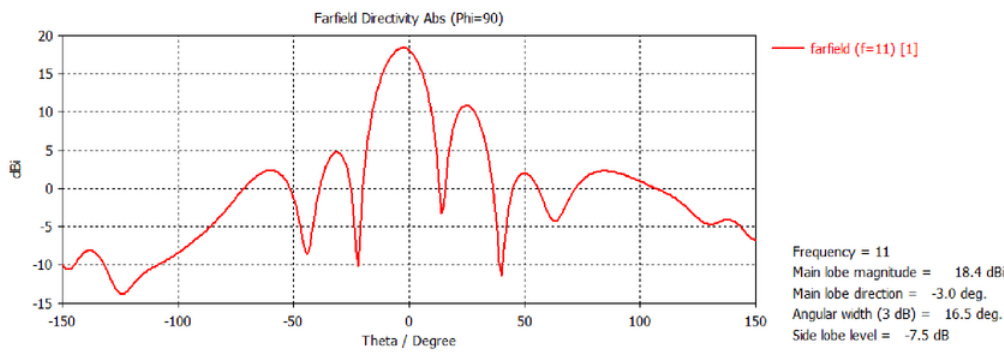


Figure 5.32: Directivity of the antenna array

The 3 dB angular width of the 4×4 antenna array was obtained as 16.5 deg which is approximately three times less than that of a single patch antenna. This means that the main lobe is narrower and focused in the broadside direction. So it increases the directivity of the antenna in to the desired direction. This result for the angular width of the array proves that the directivity of a single patch antenna can be improved by arranging it in an array.

The radiation pattern of the array indicates that its side lobe level is at -7.5 dB which is a quite high level. So, the radiation pattern is not symmetric due to this side lobe.

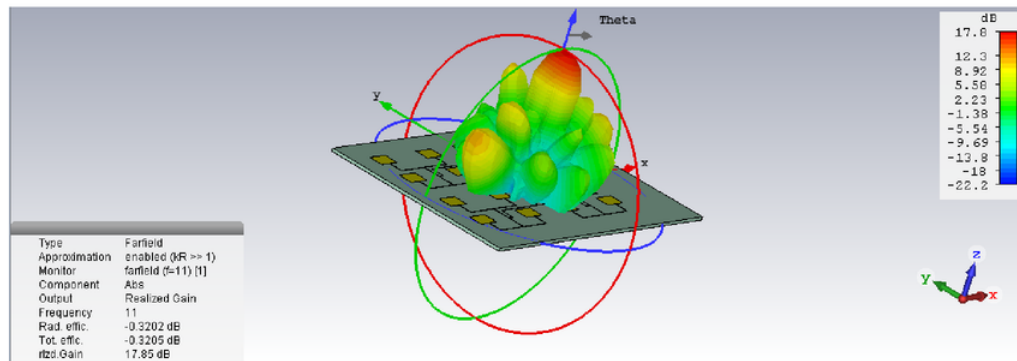


Figure 5.33: Realized gain at 11 GHz

According to the cross section of the radiation pattern in 5.34 it can be clearly seen that one edge of the antenna array radiates more than the other edge.; which means that the antenna's two radiation edges do not radiate symmetrically. Therefore it creates a higher side lobe which leads to an unsymmetrical radiation pattern.

This situation can also be explained using the power flow of the antenna array. Fig 5.35 shows the y component of the power flow. When it compares with the 3D radiation pattern, it is clear that the larger amount of power flows in to the positive theta direction where $\theta=90^\circ$. The power flow in to the opposite direction is significantly low. Therefore it can create a high side lobe in the $\theta=90^\circ$ positive theta direction which is greater than that of negative theta direction ($\theta=90^\circ$). This side lobe can be reduced if it is possible to create an infinite ground plane; but it is not possible in practice.

When an antenna array is implemented with vertically/linearly polarized patch antennas, the resulting array should also have the same polarization. The polarization of the entire antenna array can be found by investigating co-polarization and cross-polarization of its e-field. These directions are defined within spherical coordinates relating to the spherical wave fronts of a propagating EM wave. By convention, co-polarization direction refers to the direction of E-field and cross-polarization direction is the direction of H-field. The power received by a co-polarized antenna is maximum while it is minimum for cross-polarization direction. The proposed antennas array is expected to be linearly polarized so the power received in the co-plane should be higher than that of cross-plane. Fig 5.36 and Fig 5.37 shows co and cross polarizations of the e-field for $\theta=0$ and $\theta=90^\circ$ deg. In both graphs it can be clearly identified that the maximum power is received in the co-polarization direction; which means that the antenna array is vertically polarized. Therefore, if the transmitter is circularly polarized, the receiving antenna should also have the same polarization to avoid power wastage and to receive the signal properly. If the receiver is linearly polarized, it only receives the vertical components of the incoming

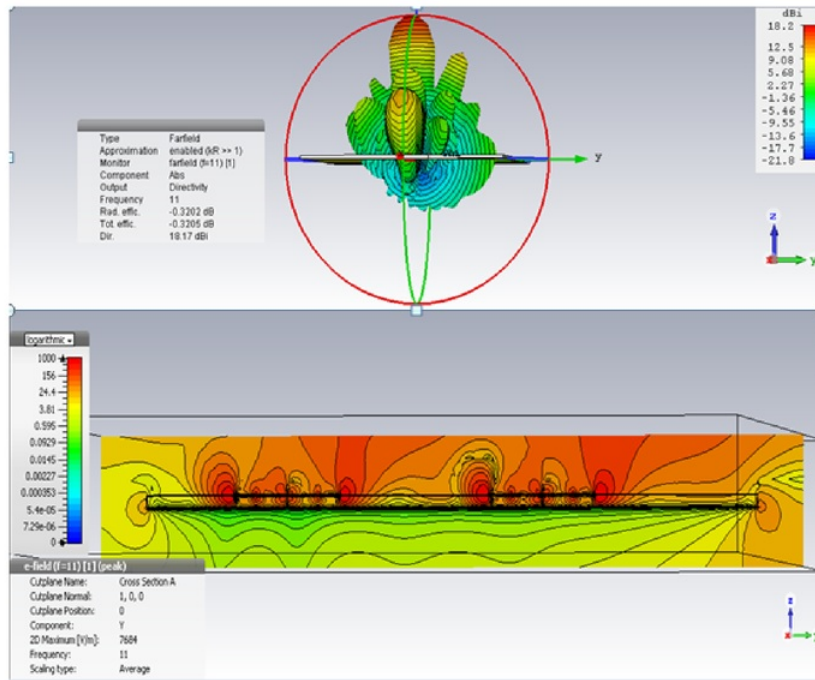


Figure 5.34: Unsymmetrical radiation from the edge of the antenna and resulting side lobe

signal. Furthermore the performance of the antenna array can be improved by minimizing the e-field in the cross plane.

5.5.2 The 4×4 array with wave-guide port

As discussed in the previous section, the initial design of the 4×4 array was done by considering the input impedance as 200Ω ; but in practice the input impedance is considered as 50Ω which is the port impedance of the network analyser. Therefore the array was modified in order to match the impedance with network analyser.

First, another quarter wavelength transformer was designed at the end of the 200Ω transmission line where the discrete port was located. It matched the 200Ω impedance of the transmission line with 50Ω port impedance. Then a waveguide port was added at the end of the quarter wavelength transformer instead of a discrete port 5.38. The width and length of the transformer had to be tuned in order to achieve the impedance matching.

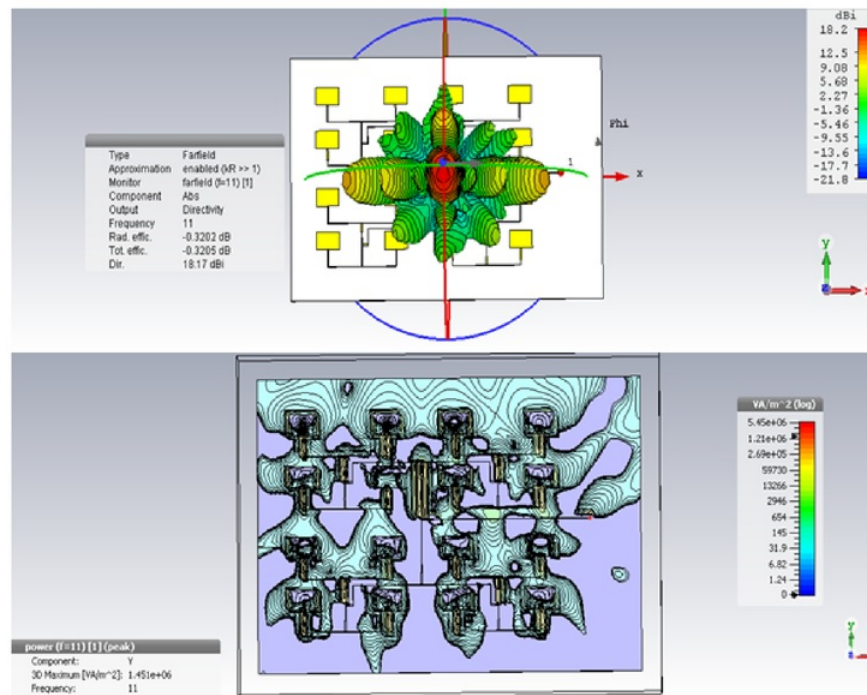
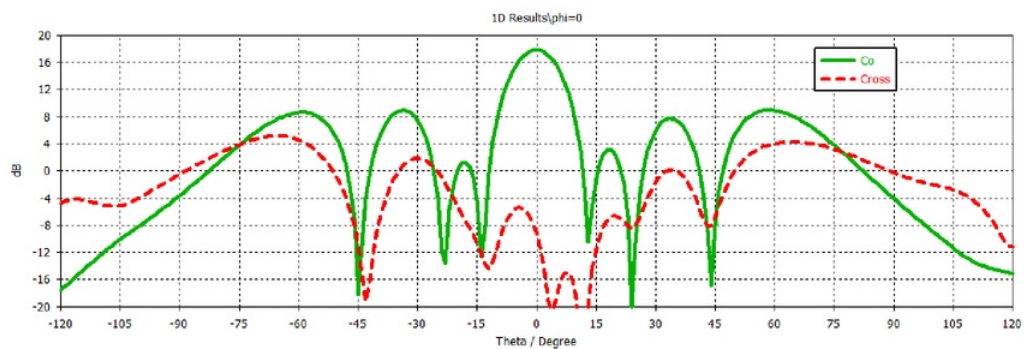


Figure 5.35: Power flow of the antenna array

Figure 5.36: Co and Cross polarization along $\phi=0$ direction

simulation results

The reflection coefficient of the antenna array was obtained as -18.6 dBi at resonance frequency 5.39. It indicates that the power radiated back by the array with waveguide

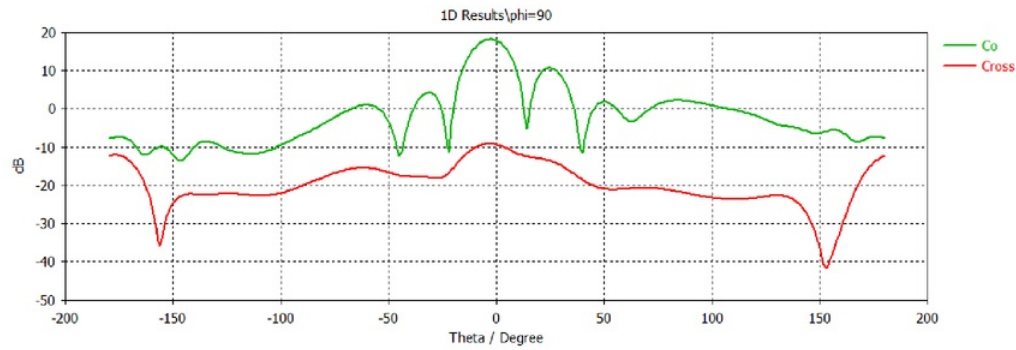


Figure 5.37: Co and Cross polarization along $\phi=90$ deg. direction

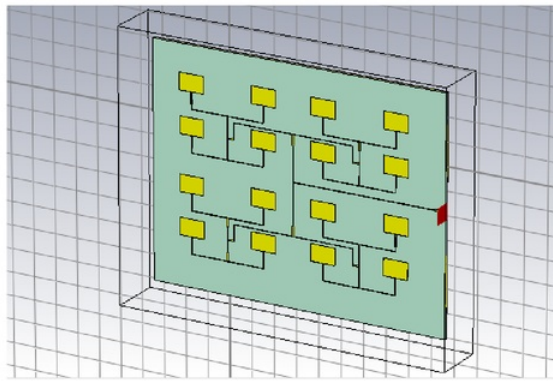


Figure 5.38: Antenna array with waveguide port

port is considerably less than what was received by the array. The VSWR which is less than 2 shows that the array is impedance matched as expected 5.40.

The directivity and the gain of the array have increased slightly to 18.7 dBi and 18 dB respectively 5.41 5.42; but the side lobe level has not changed significantly.

5.6 Prototyping and testing

After confirming the functionality of the three dimensional model of the antenna array, it can be fabricated in order to obtain the actual gain and directivity. These results can be then used to compare with the simulation results. This project also aimed to fabricate

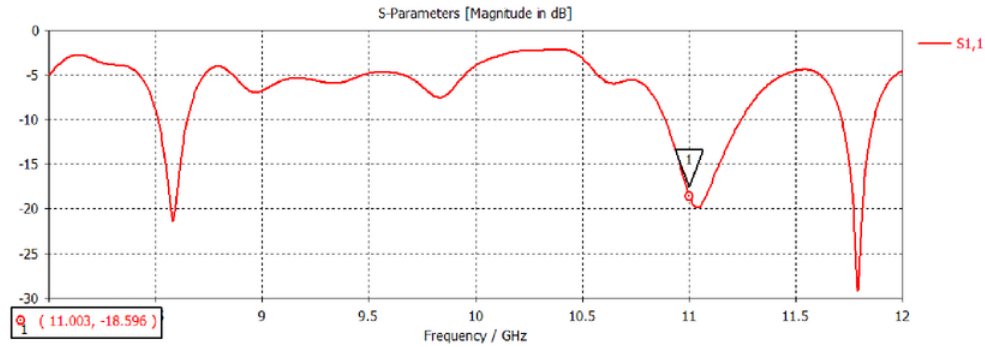


Figure 5.39: Reflection coefficient at 11 GHz

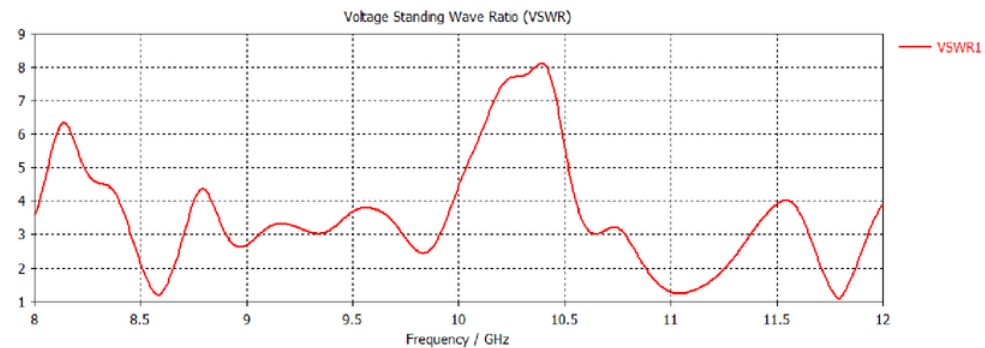


Figure 5.40: VSWR at 11 GHz

the antenna after 3D modelling but it was decided to omit the fabrication due to some constrains.

5.6.1 Budgetary constrains

One of the major constrains for the fabrication was that the cost of fabrication. The quotations from several fabricators were requested in order to select the least expensive option as the total budget for the project is limited to AUD 400. The price quotations were requested for both conditions where the fabricator uses its own material and when they uses customer material. This is because; it was aiming to use another substrate with same permittivity if the intended substrate R5880 is too expensive. The TLY-5 substrate which has the same permittivity as R5880 was expected to use if required as

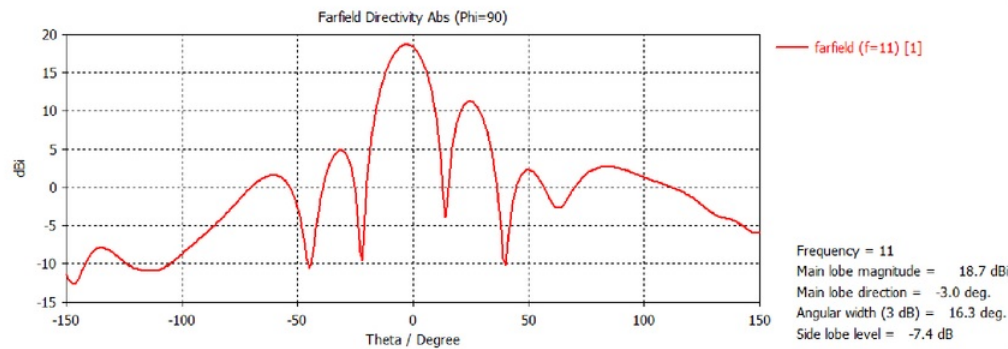


Figure 5.41: Directivity of the array at 11 GHz

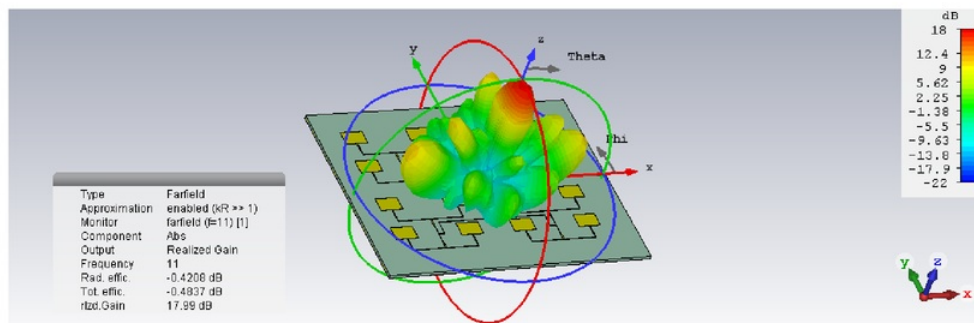


Figure 5.42: Realized gain of the array at 11 GHz

the co-supervisor had a sample from a previous project.

The price quotations were requested from LINTEK, Entech and Macquarie University Technical Services (MET). The Gerber file of the antenna array was requested from fabricators to get the accurate design parameters for the price quotation. The Gerber file creates two dimensional model of the array design which can be read by the milling machine. The CST software allows to transform these 3D models in to Gerber files.

According to the design parameters of the antenna array, the minimum width of a transmission line is approximately 0.16mm. After examining the schematic, the MET informed that it will not be able to fabricate the antenna as transmission line is too small than what it is capable of fabricating. Also the fabricating facility was not available for few weeks due to lack of fabricators.

The price quotation received from LINREK had quoted that the fabrication will cost

approximately AUD 480 if the material is provided by the customer. If not it will cost more than AUD 750. Also the minimum quantity of the order is constrained to 2 although this project required only one prototype. Furthermore, it was acknowledged that the price will not be changed although the order quantity is one.

According to the price quotation received from Entech, the cost of fabrication for the antenna array is AUD 1678 for 2 PCB boards. If the fabrication is done using customer material it costs only AUD 200 which is more cost effective. As informed, the PCB will be dispatched after 13 days therefore if the customer material was used it will take more time including the time taken to receive the material.

In addition, it was decided to get price quotation from a company from China which is known for low cost fabrication; but it was informed that the required substrate types are currently out of stock.

5.6.2 Anechoic Chamber

The Anechoic chamber 5.43 is a non-reflective echo free room which absorbs reflections of sound or electromagnetic wave. Also these chambers are isolated from waves that are entering from the outside. They are commonly used for measuring transfer functions of loudspeakers or the directivity of industry machineries. The Radio-Frequency chambers are used for testing radiating devices such as antennas and radars. The interior of RF chambers are made of radiation absorbent material and it is equipped with devices to measure the antenna radiation patterns [30].

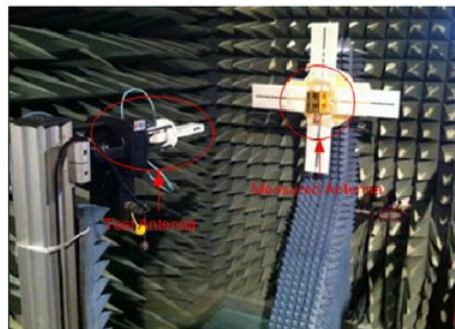


Figure 5.43: Anechoic Chamber [30]

Therefore a RF chamber can be used to test the prototype of the proposed antenna array. It allows to measure the reflection coefficient, directivity and radiation pattern of the antenna. The Macquarie University Engineering department has free access to the

RF chamber in CSIRO ICT center. The availability of the RF chamber was checked while requesting the price quotations from fabricating companies to ensure that the chamber is in operating condition. But it was informed that the chamber is not currently available for conducting experiments due to some maintenance purposes. Therefore it was decided to omit the fabrication of the antenna array after discussing with project supervisors.

Chapter 6

Beam Steering

As it was decided to skip the fabrication of the antennas array, the project was extended to investigate about beam steering of simple 1D arrays.

The beam steering is refers to changing the direction of the main lobe of an antenna's radiation pattern. In general a beam steering can be achieved by switching antenna elements or by varying the phases of the RF signals that drive antenna elements. Phased antenna arrays can be considered as the most popular application of beam steering. They are computer controlled antenna arrays which allow their beams to be electronically steered to point in various directions without physically moving the antenna elements. These phased antenna arrays are highly used in electronic engineering applications such as telecommunication and radar systems [25].

In this section a simple 1D antenna array with 4 elements is used to model the beam steering 6.1. The width and length of each patch were set to 10.78 mm and 7.3 mm respectively such that the array operates at 11 GHz. The each antenna element was fed at the edge using a discrete port. In addition the spacing between patch antennas were set to $\lambda_0/2$. Here the beam steering was tested by using the second method which varies the phase of the RF signal.

Then the array design was simulated to obtain the radiation patterns. In this case, the simulation method is bit different to what was done so far. Previously, the source type was selected as all ports in the simulation settings. But in order to see the beam steering, the phase of each antenna has to be changed. This can be done by selecting excitation list in the setup solver. This excitation list allows to simulate all the discrete ports simultaneously. Also the phase of antenna elements has to be set to $0, \phi, 2\phi, 3\phi$ depending on the number of elements. The ϕ is given by 6.1, Where λ_0 is the free space wave length, d is the distance between antenna elements and θ is the desired angle which the beam need to be steered.



Figure 6.1: 1D beam steering antenna array

$$\Phi = \frac{2 \times \pi}{\lambda_0} \sin \theta \quad (6.1)$$

6.1 Simulation results

In this the beam steering is modeled when θ is +16 deg and -16 deg. So the main lobe is expected to be steered to +16 degree and -16 deg from its initial $\theta = 0$ direction.

Fig 6.2 and fig 6.3 shows the Cartesian and 3D forms of the initial radiation pattern of the array without any phase shifts. The array has a realized gain of 13.3 dB and low side lobe level at -19.8 dB. In addition the radiation pattern is symmetric along the broadside direction.

When $\theta = +16$ deg, the radiation pattern was obtained as in fig 6.4 and fig 6.5. It can be clearly seen that the main lobe has shifted 16 deg along the positive θ direction. Also it shows that the side lobe level has increased to -11.7 dB and the gain has not changed.

When $\theta = -16$ deg, the radiation pattern steers 16 deg along the negative θ direction as shown in fig 6.6 and fig 6.6. The gain and the side lobe level of the beam steered antenna array have not changed although the angle of steering changes.

The cross section of the E-field of the -16 degree beam steered array has shown in fig 6.8 It clearly indicates that the E-field pattern has steered from the broadside direction. The CST software allows to animate this E-field pattern providing a better visualization for beam steering.

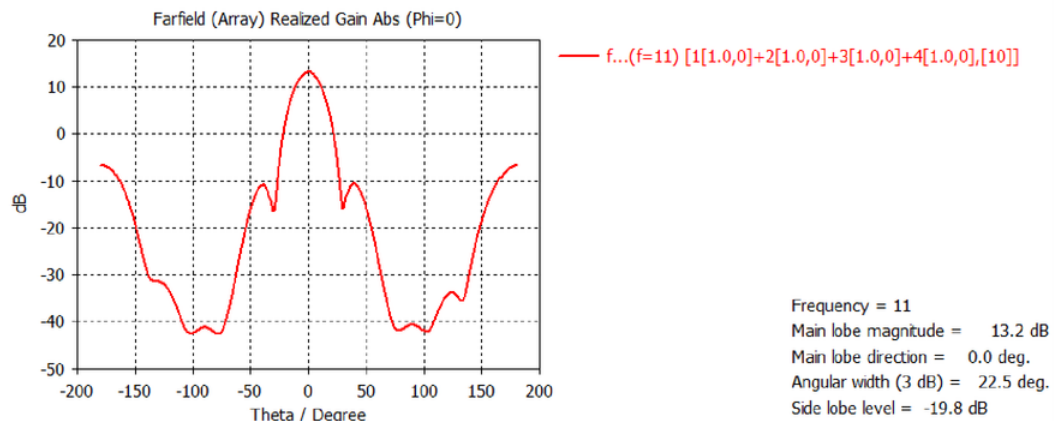


Figure 6.2: Cartesian form of the radiation pattern without beam steering

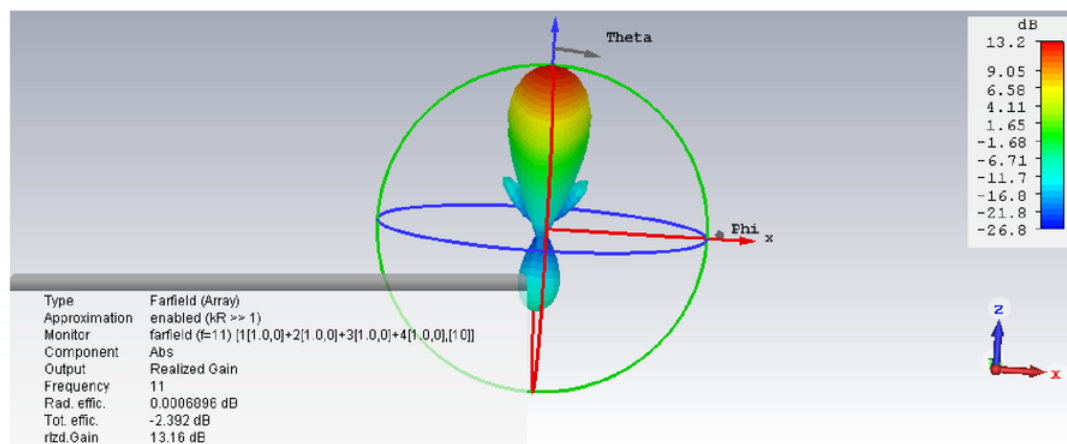
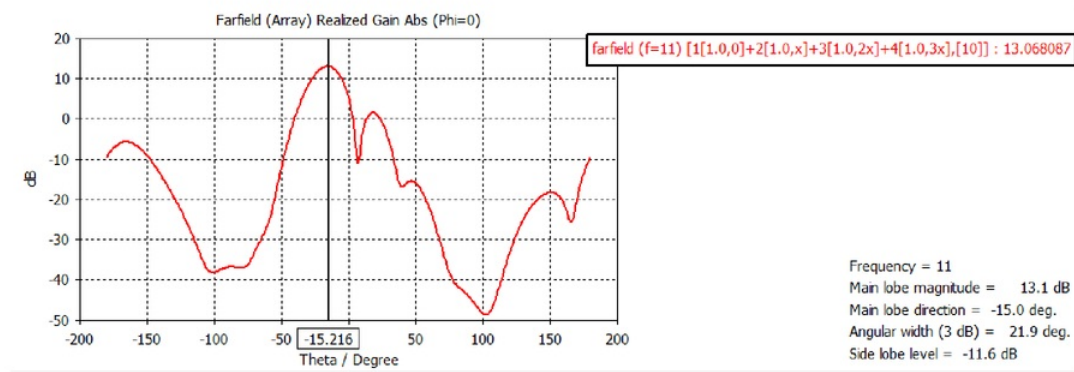
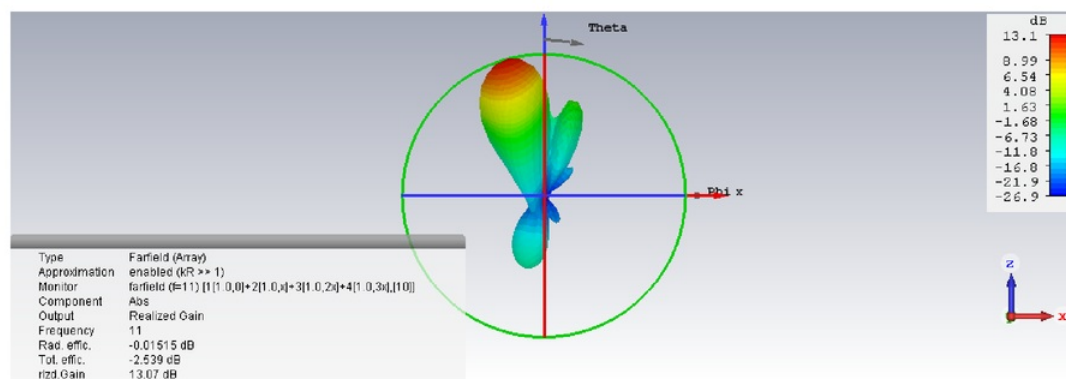


Figure 6.3: Initial 3D radiation pattern without beam steering

According to the above radiation patterns it can be concluded that the direction of the main lobe can be steered in to a desired direction by varying the phases of antenna elements. Furthermore this antenna array can be modified to obtain a phase antenna array which steers the beam electronically 6.9. The phased antenna array is fed power through phase shifters which are controlled by a computer program. This computer program alters the phase electronically allowing to steer the beam in to a different direction.

Figure 6.4: Shifted main lobe when $\theta=+16$ degFigure 6.5: Beam steering when $\theta=+16$ deg

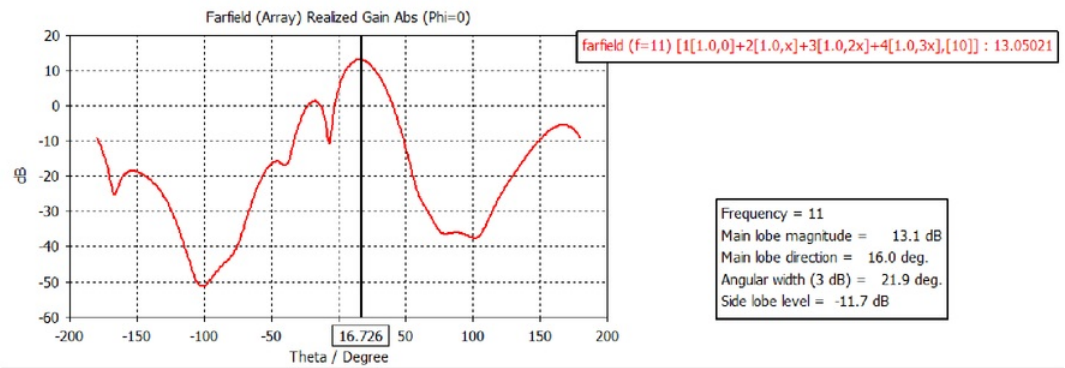


Figure 6.6: Shifted main lobe when $\theta=-16$ deg

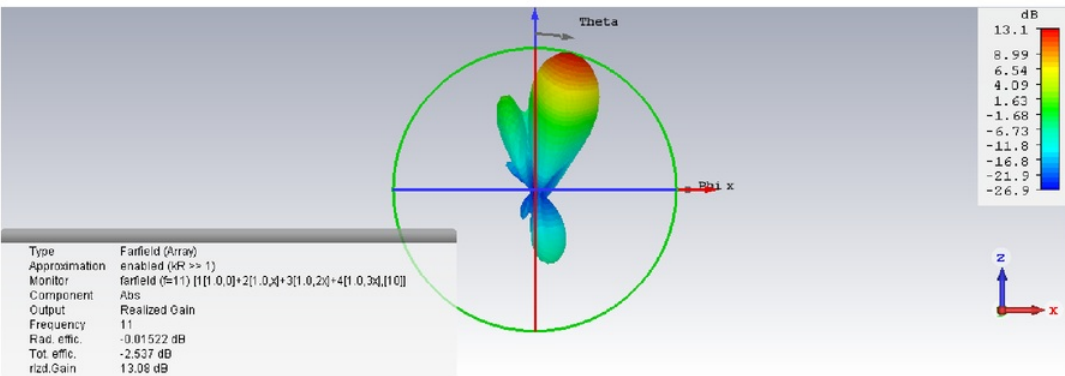


Figure 6.7: Beam steering when $\theta=-16$ deg

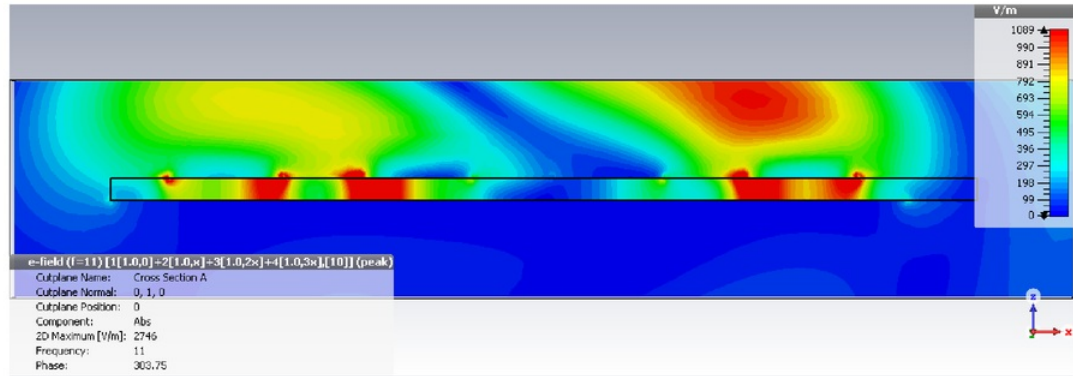


Figure 6.8: Steering of the E-field

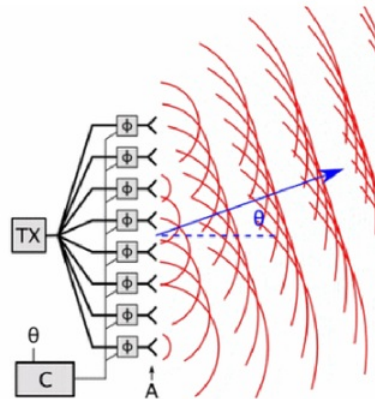


Figure 6.9: Phased antenna array [24]

Chapter 7

Conclusions and Future Work

7.1 Conclusion

This project was conducted in order to achieve a high gain and directivity of an antenna array which is targeted for long distance communication. The array development was stated by modeling a single micro-strip patch antenna in CST. The dimensions of the patch antenna depend on operating frequency, dielectric constant and the height of the substrate which it will be built on. This design uses edge feeding method as it does not require to find impedance matching point like in inset method. In this case, a quarter wavelength transformer is used to match the impedance between edge of the patch antenna and the transmission line. The length of the transformer should be set to $\lambda_g/4$ in order to achieve the required impedance matching. The optimizer tools in CST software allow to vary the other design parameters of the patch antenna to achieve the desired results at operating frequency. According to the e-field and the power flow of the single patch antenna, it is clear that the length of the patch is the critical factor when tuning its dimensions. Furthermore, the e-field is always perpendicular to the h-field of the antenna. Also the e-field pattern shows that this antenna is linearly polarized and radiates in the broadside direction. Farfield arrays can be used to select the initial element spacing of an antenna array which helps to achieve a high gain and directivity. It can be further confirmed by designing an ideal array with chosen element spacing.

The 4×4 array was developed using three sub arrays; 2×1 , 2×2 and 2×4 arrays. According to farfield results, it can be clearly seen that the gain of the antenna array increases with the number of elements in the array. Therefore it can be concluded that the realized gain of a single patch antenna can be increased by arranging it in an array. In addition, the gain of the antenna is always less than its directivity as it considers radiation losses. The angular width of the 4×4 antenna array is significantly smaller than that of single patch antenna. It means that the main lobe is narrower and more focused in the broadside direction. According to simulation results, the directivity of the antenna array is greater than that of single element. Therefore it confirms that the directivity of the antenna increases when the angular width decreases. It was noticed that the achieved

realized gain of 4×4 array is less than its expected gain due to side lobes of the radiation pattern. So the gain and the directivity of the array can be reduced by reducing the side lobe level. The reflection coefficient of the array which is significantly lower than 10 dB, guarantees that the antenna receives most of the power and less amount is reflected back. It indicates that the array is impedance matched as expected. The e-filed of the 4×4 antenna array shows that it is linearly polarized. Therefore if an antenna array is designed using linearly polarized patch antennas, it will also have the same polarization as a single antenna element. A linearly polarized receiver can only receive the vertical component of an incoming signal. Within a communication system, it is important to use a circularly polarized receiver if the transmitter is circularly polarized or if its polarization is unknown. A linearly polarized receiver is suitable only when both the receiver and transmitter are linearly polarized. The radiation pattern of the 4×4 array has a side lobe at a quite high level due to unsymmetrical radiation along its edges. It can be reduced by increasing the size of the ground plane. It is important to optimize the array in each development stage as it helps to achieve the desired results by tuning fewer amount of design parameters. The size of the antenna array could minimize as expected improving its area efficiency.

In terms of fabricating the array, it is important to consider the budgetary constraints when selecting the substrate for the array design. It was noticed that the substrate used for this project is quite expensive than others. It should also consider the fabricating capability of the fabricators as they may have some limitations.

The beam steering arrays allow to steer the main lobe of a radiation pattern in to a desired direction. They can be further modified to implement phased antenna arrays which electronically steer the beam without physical moving the array.

7.2 Future Work

The ultimate goal of this project was to design a model of 4×4 antenna array that has a high gain and directivity. The performance of the 3D model was investigated based on its characteristics such as reflection coefficient, VSWR and properties of farfield radiation pattern. These characteristics were minimized or maximized in each design stage depending on their effect on overall antenna performance. The desired values for these performance characteristic were achieved by varying design parameters such as widths and lengths using CST optimizer tools. So far, the simulation results guarantee that the 3D model of the 4×4 antenna array designed in CST performs as expected. The next step is to design a prototype of the array and test it in RF chamber. If the prototype performs satisfying all the design specifications it can be developed further and used for telecommunication applications. As discussed before, the prototype was not designed in this stage due to technical reasons. Therefore the future work of this project includes

implementing and testing a prototype of antenna array.

In addition, the performance of 3D model of the antenna array can be further improved by modifying its 90° bends in the feed network. In a complex feed network, the micro-strip lines necessarily happen to be turned through a large angle. An angle of 90° bend of a transmission line can lead to a significant portion of incoming signal to be reflected back. This can affect the impedance matching of a more complex antenna design as it has many bends. One method of minimizing this signal reflection is to curve the patch of the micro-strip in an arc of radius which is at least 3 times of its width. However the most common method is the mitered bend technique which consumes smaller space 7.1.

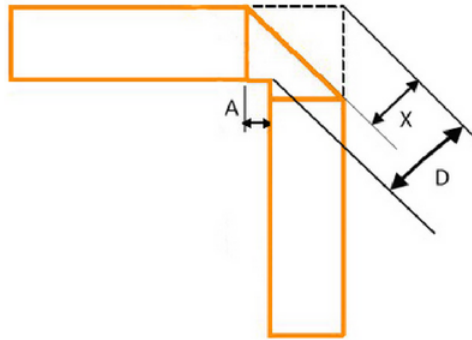


Figure 7.1: Mitered bend technique

Although the 3D model works perfectly with 90° bends, using mitered bends is more practical if the project is aiming to design a prototype of the array. Therefore it will be better if the model is modified with mitered bends before fabrication.

Furthermore, the prototype of the 1D beam steering antenna array can be designed and tested. Then it can be modified to perform as a phased antenna array. The 4×4 antenna array can also be modified to a phased array in order to use in applications such as radar systems.



Chapter 8



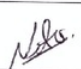

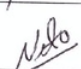

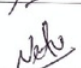

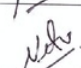

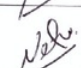



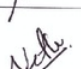





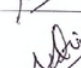

Abbreviations

MIMO	Multiple-Input and Multiple-Output
GPS	Global positioning satellite systems
NASA	National Aeronautics and Space Administration
SMA	Microstrip subMiniature version A
VSWR	Voltage Standing Wave Ratio







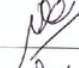

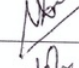

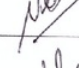

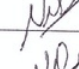

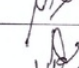

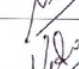

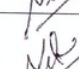

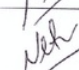

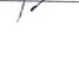

Appendix A

Attendance Form

Consultation Meetings Attendance Form

Week	Date	Comments (if applicable)	Student's Signature	Supervisor's Signature
Winter Holidays	06/07/17	Discussed about project plan and how to start the antenna design.		
Winter Holidays	07/07/17	Probe feed and transmission line feed technique.		
Winter Holidays	20/07/17	It was decided to use 'Probe feed method to do simulation of the patch.		
Winter Holidays	27/07/17	Discussed about smith charts and array configurations.		
Week 1	02/08/17	It was advised to use far-field arrays to check spacing of arrays.		
Week 2	07/08/17	It was decided to start feed network designing with a two-way splitter.		
Week 3	15/08/17	Impedance matching of the feed network.		
Week 3	16/08/17	Two way splitter's parameters.		
Week 3	18/08/17	Progress report structure calculations of array arrangement.		
Week 4	25/08/17	Edge impedance calculating and impedance transformer.		
Week 5	31/08/17	Discussed about designs of ideal array (16x16) design.		

Consultation Meetings Attendance Form

Week	Date	Comments (if applicable)	Student's Signature	Supervisor's Signature
Week 6	07/09/17	single patch antenna design.		
Week 6	10/09/17	2x1 array design and discussion.		
Week 7	15/09/17	2x2 array design and discussion.		
Week 7	18/09/17	2x4 array design.		
mid Semester	21/09/17	4x4 array design and impedance matching.		
mid semester	26/09/17	4x4 array array design (reducing side lobes and improving directivity).		
mid semester	29/09/17.	Modifying the final antenna array with a waveguide port.		
Week 8	4/10/17	Discussed about designing SMA connectors in CST.		
Week 9	12/10/17	Discussed and compared the price quotes received from fabricators.		
Week 10	17/10/17	Contacting checking checked availability of RF chamber.		
Week 11	24/10/17	explained about Beam steering and phased array.		
Week 11	25/10/17.	designing a 1D array to examine beam steering.		

[illegible]

References

- [1] W.D. Bliss and G. Siddartan, *Adaptive Wireless Communications: MIMO Channels and Networks*. Cambridge: Cambridge University Press, 2013, pp.170-200.
- [2] N. Aleksandar, R. Lvana, M. Zoran and J. Sinha, Side lobe suspension of printed antenna array for integration with microwave circuits, *Microwave Journal*, vol.53, p.72, 2010.
- [3] G.Ovejero, F.Mesa and C.Craeye, Accelerated macro basis functions analysis of finite printed antenna arrays through 2D and 3D multiple expansions, *IEEE Transactions on Antennas and Propagation*, vol.61, p.707, 2013.
- [4] C.A. Balanis, *Antenna theory: analysis and design*. New York: Harper and Row, 1982.
- [5] Antenna array [online]. Available: https://en.wikipedia.org/wiki/Antenna_array
- [6] Micro strip antenna [Online]. Available: https://en.wikipedia.org/wiki/Microstrip_antenna
- [7] J.P.Santos, J.M. Kovitz, and Y.R. Sammii (2015, Aug). *Talking To MarsNew Antenna Design Will Aid Interplanetary Communication* [Online]. Available:<https://phys.org/news/2015-08-marsnew-antenna-aid-interplanetary.html>
- [8] K. Lee, "A personal overview of the development of micro strip patch antennas", IEEE Conferences, 2016
- [9] J. Saini and S.K. Agrawal, Design a single Band Micro strip Patch Antenna at 60 GHZ Millimeter Wave for 5G Application, International Conference on Computer, Communication and Electronics, Manipal University, Jaipur, 2017.
- [10] D. Prabhakar, P. M. Rao and M. Satyanarayana, "Design of rectangular pacth antenna array with multiple slots by using mitered bend feed network for multi-bend feed network for multi-band application", International Conference on ElectroMagnetic Interference and Compatibility, 2016.
- [11] Beenish, T. Saraswati and et.al, "Design of a high gain 16 element array of micro strip patch antennas for millimetre wave applications", 2016 2nd International Conference on Contemporary and Informatics, Uttar pardesh, pp. 182-184 , 2016

- [12] O. U. Khan, "Design of 4×4 Butler Matrix for Microstrip Patch Antenna Array", TENCON 2006-2006 IEEE Region 10 Conference, 2006.
- [13] S.G. Zhou, P. Dong and et.al, "Wideband Antenna Array With Full Metal structure and Air-Filled Micro strip Feeding Network", *IEEE Transactions on Antennas and Propagation*, vol.65, pp.3041-3049, 2017.
- [14] H.M. Lee, "Pattern Reconfigurable Micro-strip Patch Array Antenna using Switchable Feed-Network", Proceeding of Asia-Pacific Microwave Conference, 2010
- [15] Micro Strip Patch Antenna Calculator [Online]. Available : <https://www.pasternack.com/t-calculator-microstrip-ant.aspx>
- [16] Micro Strip line Calculator [Online]: Available: <http://www.emtalk.com/mscalc.php>
- [17] B.S. Singh and K.P.Ray, "A compact modified corporate feed network for antenna array with non-identical rectangular microstrip antenna elements", International Symposium on Antenna Propagation, Mumbai, 2016
- [18]] N.J. Shimu and A. Ahmed, "Design and performance analysis of rectangular microstrip patch antenna at 2.45 GHz", 5th International Conference on Informatics, Electronics and Vision, Bangladesh, 2016
- [19] R.Kiruthika and T. Shanmuganantham, "Comparison of Different Shapes in Microstrip Patch Antenna for X-band Applications", International Conference on Emerging Technological Trends, 2016
- [20] R. Widiandari and A. Munir "Proximity coupled X-band patch antenna array with dual polarization", International Electronic Symposium, Indonesia, 2016
- [21] M. U. Afzal and K. P. Esselle, "Steering the beam of medium-to-high gain antennas using near-field phase transformation", *IEEE Trans. Antennas and Propagation*, vol. 65, no. 4, pp. 1680-1690, April 2017
- [22] Z. Yu-wei, L. Shu and et.al, "The simulation design of low-side lobe level high gain and broadband microstrip patch antenna array", ISAP conference, Okinawa, 2016
- [23] G. Ahmad, "Design, optimization and development of X-band microstrip patch antenna array for high gain, low sidelobes and impedance matching", Second International Conference on Electrical Engineering, Lahore, 2008
- [24] Antenna Theory [Online]. Available: <http://www.antenna-theory.com/antennas/patches/patch3.php>
- [25] I.Uchendu and J.Kelly, "Survey of Beam steering Techniques Available for Millimeter Wave Applications", *Progress In Electromagnetic Research*, vol.68, pp.35-54, 2016

-
- [26] CST MICROWAVE STUDIO [Online]. Available:<http://www.cst.com/products/cstmws>
- [27] X. Qi, L.Xiaowu and S. Zhanjun, "Analysis of the directivity of pattern-steerable short-wave-limb delta antenna", Asia-pasific Microwave Conference Proceeings, 2005
- [28] Radiation Pattern [Online]. Available:<http://www.antenna-theory.com/basics/radpattern.php>
- [29] Microstrip Quarter wave transformer [Online]. Available:<https://www.cst.com/academia/examples/quarter-wave-transformer>
- [30] Anechoic Chamber [Online]: Available:https://en.wikipedia.org/wiki/Anechoic_chamber